Proton MRS Can Determine the Pathology of Human Cancers with a High Level of Accuracy

Carolyn E. Mountford,* Sinead Doran, Cynthia L. Lean, and Peter Russell

Institute for Magnetic Resonance Research, P.O. Box 148, St. Leonards, 1590 NSW, and Department of Magnetic Resonance in Medicine, University of Sydney, NSW, Australia

Received November 6, 2003

Contents

* To whom correspondence should be addressed at the Institute for Magnetic Resonance Research. Phone: 61 2 9926 6073. Fax: 61 2 9926 6549. E-mail: caro@imrr.usyd.edu.au.

1. Introduction

1.1. History

The first report of a high-resolution proton (^{1}H) magnetic resonance spectrum from intact viable cancer cells was made by Block and colleagues in 1973,[1] who suggested ^{1}H magnetic resonance spectroscopy (MRS) might lead to pathologically relevant information. However, at this time ^{1}H was not the favored nucleus since adequate water suppression was difficult and small resonances were swamped by a much larger water signal. Carbon-13 (^{13}C) MRS[2] and phosphorus-31 (^{31}P) MRS[3] were the preferred methods for monitoring cellular metabolism and intact viable cells and organs.

The musings of two Oxford dons in 1975 convinced C.E.M. to spend the last 28 years on the topic of this review. Professor R. J. P. Williams, an inorganic chemist, was convinced that MRS would revolutionize biology and medicine. He spent his Sundays picking berries and seeds to put in the magnet the following day. He and his group produced the first ^{1}H spectra of the adrenal gland of the rat.[4] Professor Rodney Porter, the 1972 Nobel laureate for immunology, repeatedly stated that diseased cells had a much higher chemical activity than healthy cells. If both of these scientists were indeed correct, then MRS had the potential to assist in the pathological diagnosis of human diseases.

A series of experiments undertaken in Sydney in 1978 indicated that MRS could identify the sequential or stepwise alterations in cells prior to them manifesting frank malignancy, by light microscopy. The AKR mouse model, developed by Professor Don Metcalf in Melbourne, was an inbred strain of mice with a virus transmitted genetically which results in a spontaneously developing T-cell leukemia. The disease first develops in the thymus.[5] MR spectral differences were recorded from the thymus, indicating that the chemical composition of the cells changed prior to such changes being identifiable cytologically or histologically. MRS measured a continuum of changes taking place in the thymus as the final preleukemic period ended and neoplasia occurred.[6,7]

Using a mouse model developed by Dr. Ian Ramshaw in Canberra,[8] it was subsequently demonstrated that ^{1}H MRS distinguished between tumor

10.1021/cr030410g CCC: $48.50
Published on Web 08/11/2004

Carolyn E. Mountford obtained her Doctor of Philosophy degree from Sommerville College, Oxford, specializing in biophysics and biochemistry. She has been a proponent of multidisciplinary research for over 25 years. Dr. Mountford is the Foundation Chief Executive of the Institute for Magnetic Resonance Research and Foundation Head of the Department of Magnetic Resonance in Medicine at the University of Sydney. Dr. Mountford is a Fellow of the International Society of Magnetic Resonance in Medicine and has honorary positions in Surgery and Radiology at the University of Sydney. She has authored well over a hundred peer-reviewed articles, book chapters, and textbooks and has been awarded the NSW Cancer Council's Inaugural "Pioneer of Hope Award" and the Royal Australasian College of Surgeons' Graham Coupland Medal. As a member of the Australian Science Engineering and Technology Council, Dr. Mountford chaired the ASTEC study for the development of guidelines for the ethics and scientific management of Australian world heritage and protected areas.

Cynthia L. Lean is Scientific Director, Post-graduate Coordinator, and Deputy Chief Executive of the Institute for Magnetic Resonance Research and Deputy Head of the Department of Magnetic Resonance in Medicine at the University of Sydney. Dr. Lean is a scientist with a background in chemistry and biochemistry investigating the use of magnetic resonance spectroscopy for the early detection and diagnosis of cancer. Following completion of her Ph.D. at the Department of Medicine, University of Sydney, she was awarded a research fellowship at the NMR Center, Massachusetts General Hospital (MGH), Harvard Medical School, for 1994–5. At MGH, Dr. Lean incorporated her expertise in the application of MR to tumor development and progression and helped develop a new and improved means of early cancer detection using a technique called magic angle spinning MRS. Dr. Lean now works with a team of scientists, surgeons, pathologists. and graduate students developing magnetic resonance as an adjunct to and in some cases a replacement for histopathology in the early detection of cancer.

Sinead Doran is a senior scientist at the Institute for Magnetic Resonance Research, specializing in *ex vivo* and *in vivo* spectroscopy. Ms. Doran completed a Higher National Diploma in applied sciences with computers at Luton University in 1989 and a B.Sc. (Hons) at Oxford Brookes University, Oxford, specializing in biological sciences, in 1992. Her particular areas of interest include computational methods and translation of the biopsy program into the pathology laboratory for routine use.

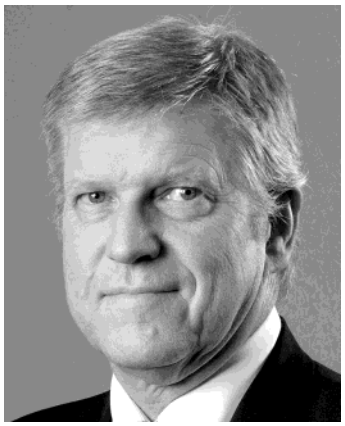

Peter Russell, M.D. (Sydney), M.B. B.S., B.Sc. (medicine), FRCPA, graduated from the University of Sydney in medical science in 1966 and in medicine in January 1968. Prof. Russell obtained his Fellowship of the Royal College of Pathologists of Australasia in 1973 (special anatomical pathology). He was appointed salaried specialist in pathology at Royal Prince Alfred Hospital in 1974 (Head of Department, 1995–2002) and obtained his M.D. at the University of Sydney in 1991 ("Pathology of Borderline Ovarian Tumours"). In 1992 he was appointed Director of Pathology at Sydney IVF and Medical Director of Laverty Pathology in November 2001. Prof. Russell has broadly based experience in gynecological histopathology with special interests in gynecological neoplasia, infertility, and pregnancy failure. His research interests are in female genital tract malignancy and reproductive pathology. He is the author of over 200 peer-reviewed articles, book chapters, and textbooks on gynecological pathology. Prof. Russell is Director of Pathology at the Institute for Magnetic Resonance Research. He has professional affiliations with the Royal College of Pathologists of Australasia, International Academy of Pathology, International Society of Gynecological Pathologists (Secretary 1986–90, Vice President 1994–96, President 1996–98), and Australian Society for Colposcopy and Cervical Pathology.

cells with a capacity to metastasize and those that produced only locally invasive tumors. Assignment of the one-dimensional (1D) MR spectra indicated multiple differences including that in the cholesterol-to-phospholipid ratio and the presence or absence of cholesterol ester. Of particular interest was a resonance with a long T_2 relaxation rate, at a chemical shift of 1.3 ppm, which clearly identified those primary tumors with a capacity to metastasize.[9−11] The assignment of the potentially diagnostic and prognostic resonances was made possible by two-dimensional (2D) MR methods.[12,13]

The capacity of MRS to determine both neoplastic status and prognostic variables from human biopsies with histological correlation approaching 100% has now been demonstrated.[14] The MR method is fast, accurate, and robust and complements routine biopsy

diagnosis. The technology was extended to *in vivo* ^{1}H MRS in the 1990s and is now in clinical use for some organs, including studying brain metabolism.

1.2. Limitations of Histopathology

Histopathology has been the medical diagnostic gold standard for much of the 20th century, providing diagnostic and prognostic information for human diseases. Histopathology is a mature discipline that draws upon many decades of experience by medical specialists who rely on pattern recognition in human tissues and cells using light microscopy.

The principal limitation to histopathology is the restricted range of morphological changes that tissues can express, each in a continuum, yet from which pathologists are expected to identify patterns specific for individual diseases. These patterns overlap and are susceptible to subjective assessment. Moreover, sampling errors, inherent at several levels in routine diagnostic services, are at least partly due to the cost of examining multiple sections of tissue. The skill, experience, and thoroughness of surgeons and pathologists play a major role in ensuring detailed diagnostic and prognostic information.

For much of the 1980s and early 1990s the accuracy of the MRS method for determining the biological status of human tissues was severely doubted. It was not understood that variation in MR spectral changes and pathological features in tissues from area to area meant that, for the correct correlation to be made, the precise piece of tissue from which the MRS signal was obtained also had to be examined by the pathologist with specialized step-sectioning of the specimen.

When P.R., a pathologist, saw the potential of the MRS method and joined the ^{1}H MRS program, the accuracy of the MRS method became clear. The detailed pathological analysis, when correlated with the MRS data, resulted in accuracies that approached 100%. In addition, the unique role of the MRS method to identify stages in a pathological process not appreciable by light microscopy, although clinically confirmed, became evident. Stated differently, there were biological states that were not morphologically manifest that could be discerned by MRS.

For the MRS method to achieve its full potential, detailed histopathological analysis of the precise piece of tissue examined by MRS was needed. This philosophy applies to both preoperative and postoperative specimens, i.e., on biopsy or on the resected organ following *in vivo* spectroscopy.

1.3. Handling of Tissue Specimens for MRS

Some who have tried to emulate the tissue biopsy studies described below have failed initially due to the methods employed to handle the specimens prior to MRS examination.

For each tissue type the handling protocols have been individually determined and reported.[15−24] The polypropylene vials that the specimens are collected in must be tested for leakage of minute levels of chemicals, which leach from the plastics and cause cell death. Similarly, for fine-needle aspiration biopsies (FNABs) the barrels of the syringes need to be tested.[25]

The specimens must be immediately placed in a vial containing PBS/D_2O after the biopsy is obtained and frozen without delay in liquid nitrogen. There is an exponential decrease in accuracy of the MRS method with the length of time the specimen is left "sitting on the bench". According to the type of tissue, there is a finite time it can be stored in the freezer before the MRS examination is undertaken, before the accuracy decreases. One group tried to repeat the thyroid study with specimens over 3 and up to 7 years old, a guaranteed recipe for failure. Another group used unsuitable plastic syringes, which lysed the cells, rendering the spectra useless.

1.4. Statistical Classification Strategy. Managing Large Volumes of Data

Magnetic resonance spectroscopy is known to report on pools of chemicals in cells and tissues as they alter (many at the same time) with aging and the development of disease processes.[15−21,26−37] Many of these biochemical processes occur in parallel, but do not necessarily alter in the same direction. Thus, managing complex databases, which include large volumes of biomedical data including spectroscopy, pathology, and patient statistics, requires a special methodology. The lack of specialist methods to overcome this problem was recognized by Dr. Ian Smith (National Research Council (NRC), Canada) in the late 1970s.

A three-stage statistical classification strategy (SCS) was developed at the Institute for Biodiagnostics (IBD), NRC, by Dr. Ian Smith and Dr. Ray Somorjai specifically to address these issues. The method has allowed automated analysis of both *ex vivo* and *in vivo* spectroscopic data using highly accurate and reliable mathematical classifiers for a variety of clinical applications. For a review see ref 14.

The application of SCS methodology provides classifiers that distinguish benign from malignant specimens with accuracies of 100% when a small proportion of samples that are unable to be accurately classified are excluded. When these samples are included, accuracies in the mid-90s (percent) can still be achieved.

Unlike most other methods, the SCS method identifies those spectral regions from which the diagnostic and prognostic information has been obtained. This allows the chemical species to be identified and the biochemical pathways involved in the disease process to be studied. Quite often the spectral region is complicated and contains many overlapping resonances. This is where the 2D spectroscopy method becomes important (see sections 3.1, 3.2, and 4.6).

MRS is now poised to supplement the already significant contribution of magnetic resonance imaging (MRI) for the clinical management of disease. As well as accurately reporting pathological processes in tissue, spectroscopy also identifies important subsets of disease states that are not morphologically manifest in either biopsy or *in vivo* imaging. The

MRS method *in vivo* is currently being developed with accuracies approaching those employing MRS on excised biopsy specimens. Many of the pitfalls found in the biopsy program exist with *in vivo* MRS, where correlations with final histological diagnosis are further confounded by the use of a lower frequency magnet and different experimental conditions.

To ensure rapid entry of these technologies into clinical practice, methods of translating them into the clinic need to be recognized and appropriate clinical acceptance testing needs to be undertaken.

Described below is the current state of MRS on biopsies and *in vivo* for neuro, prostate, thyroid, and breast spectroscopy. Finally, individual case studies are presented to demonstrate the effectiveness of MRS in the cancer clinic.

This review has been limited to describing those ^{1}H MRS studies where a significant number of biopsies or patients have been investigated. It also emphasizes and explains the capacity of MRS to identify the presence of human diseases which are not morphologically manifest and thus not observed using light microscopy.

2. 1D MRS on Biopsies

2.1. Cervix

Cancer of the uterine cervix was chosen for the first (8.5T, 360 MHz) ^{1}H MRS clinical study on human biopsies[32] as histologically the distinction between the presence and absence of malignancy is made cost-effective and with a very high level of accuracy. In the first report, spectra of 39 of 40 invasive specimens (Figure 1C) were characterized by an intense resonance at 1.33 ppm, primarily from the methylene protons of lipid acyl chains, with additional contributions from the methyl protons of lactate and threonine. There were also methyl, choline, and olefinic resonances at 0.90, 3.2, and 5.32 ppm, respectively (Table 1).

The spectrum from human papilloma virus (HPV) infected tissue (Figure 1B) lacked the intense methylene resonance at 1.33 ppm. Other visible spectral differences included increases in the broad, featureless resonance between 3.4 and 4.2 ppm in preinvasive specimens, compared with their invasive counterparts.

The spectrum shown in Figure 1A is from a piece of tissue containing a chronic inflammatory cell infiltrate with no features of HPV infection or dysplasia.

When the CH_2/CH_3 ratio was plotted against the CH/CH_2 ratio to compare the premalignant states with invasive carcinoma (Figure 2), a separation between invasive and preinvasive cells was achieved with a sensitivity and specificity of 94% and 98%, respectively.[17] Thus, ^{1}H MRS was able to distinguish between preinvasive and invasive cervical cancer *ex vivo*, based on the detection of altered invasive-cell chemistry.

Such gradational changes suggest that the two working hypotheses of Professors Williams and Porter were correct, with increasing chemical activity becoming apparent as the disease's process progresses.

A further advantage of the 1D MRS method is that it examines the entire biopsy specimen and leaves

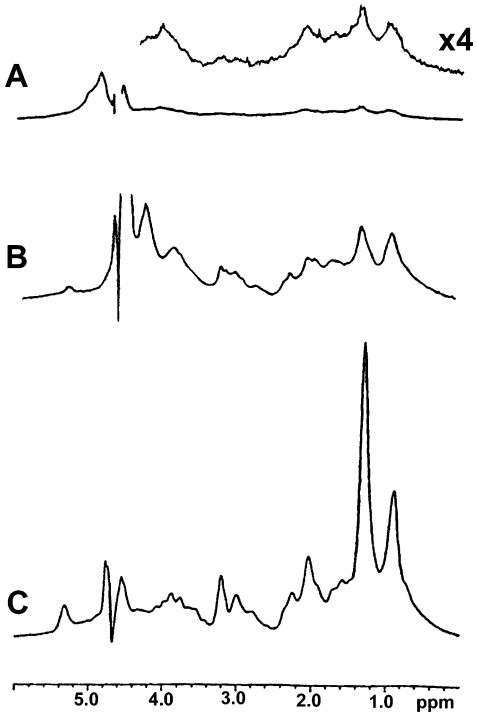

Figure 1. ^{1}H MR spectra of cervical biopsy specimens. The histological assessment of each specimen is as follows: (A) nonspecific chronic inflammatory disease (the inset shows the 4.5−0 ppm region with the vertical gain increased 4-fold; NE = 400); (B) HPV infection but no significant dysplasia observed, 512 accumulations; (C) cervical carcinoma, 40 accumulations. The spectra were recorded on a Bruker WM 400 (9.4T) spectrometer at 37 °C. The water peak was suppressed by gated irradiation, sweep width 4000 Hz, acquisition time 1.024 s, and a line broadening of 3 Hz was applied in each case. Reprinted with permission from ref 32. Copyright 1990 Wiley-Liss, Inc., a subsidiary of John Wiley & Sons, Inc.

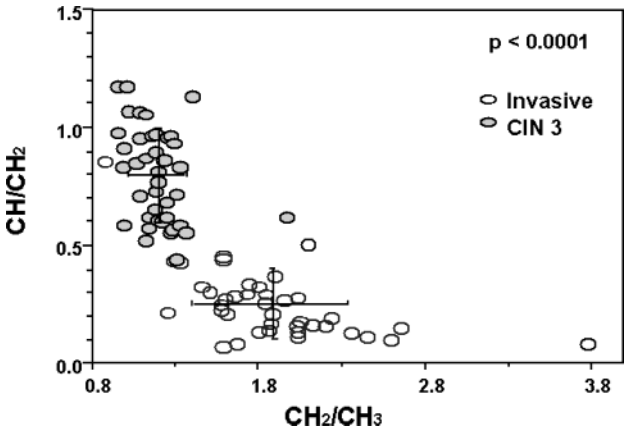

Figure 2. Peak height ratios from MR spectra from cervix biopsies. Two ratios are plotted on the same graph, the ratio of the CH/CH_2 resonances versus the ratio of the CH_2/CH_3 resonances. The graph compares one of the higher grade dyplastic states—CIN 3 with invasive carcinoma. The cross hairs show the mean ± standard deviation for each category. A Student's t test gives $P < 0.0001$ for CH/CH_2 and CH_2/CH_3. Reprinted with permission from ref 17. Copyright 1993 Radiological Society of North America.

Table 1: Resonances in One-Dimensional ^{1}H MR Spectra

molecule	abbrev	species	resonance assignment (ppm)
		Amines	
choline, phosphocholine, glycerophosphocholine	Chol	$-N(C\mathbf{H}_3)_3$	3.2
spermine, spermidine, polyamines	PA	$-NC\mathbf{H}_2$	3.1
creatine, phosphocreatine	Cr	$-NC\mathbf{H}_3$	3.0
		Lipids	
triaclglycerol (fatty acyl chain)	Lip	$C\mathbf{H}_3CH_2CH_2-$	0.90
	Lip	$CH_3C\mathbf{H}_2CH_2-$	1.33
	Lip	$-OOCCH_2C\mathbf{H}_2$	1.6−1.7
	Lip	$CH_3C\mathbf{H}_2CH_2-$	2.02
	Lip	$CH{=}CHC\mathbf{H}_2-$	2.08
	Lip	$-OOCC\mathbf{H}_2CH_2$	2.3
	Lip	$C\mathbf{H}{=}CH-$	5.32
		Amino Acids	
alanine	Ala	$-C\mathbf{H}_3CH-$	1.49
glutamate, glutamine	Glu, Gln	$-CHC\mathbf{H}_2CH_2COO^-/NH_3^+$	2.2
glutamate, glutamine	Glu, Gln	$-CHC\mathbf{H}_2CH_2COO^-/NH_3^+$	2.6
isoleucine	Ile	$-C\mathbf{H}_3$	0.97
leucine	Leu	$-C\mathbf{H}_3$	0.97
lysine	Lys	$H_3N^+CH_2C\mathbf{H}_2CH_2$	1.7
lysine	Lys	$H_3N^+CH_2C\mathbf{H}_2CH_2$	3.03
threonine	Thr	$C\mathbf{H}_3CHOH-$	1.33
threonine	Thr	$C\mathbf{H}_3CHOH-$	4.25
valine	Val	$-C\mathbf{H}_3$	1.03
		Other	
lactate	Lac	$-C\mathbf{H}_3CH-$	1.33
citrate	Cit	$-OOCC\mathbf{H}_A\mathbf{H}_BC(OH)$	2.4−2.7
taurine	Tau	$H_3N^+C\mathbf{H}_2CH_2SO_3^-$	3.25
taurine	Tau	$H_3N^+C\mathbf{H}_2CH_2SO_3^-$	3.43

the tissue intact for further histologic assessment. Current taxonomy divides preinvasive cervical dysplasia or cervical intraepithelial neoplasia (CIN) into three categories. It is arguable whether these changes are a progressive spectrum or different disease entities. Interestingly, neither visual inspection of MRS data nor the application of SCS to the spectra from preinvasive cervical tissues CIN I, CIN II, and CIN III (Smith and Somorjai, unpublished data) provided a clear delineation. It is quite arbitrary histologically to definitively distinguish between these categories as they overlap in any given tissue sample, and variation may be more apparent than real. Thus, improved analysis methods are needed to allow the precise volume of each histological pattern to be evaluated in each spectrum. The new mathematical regression method developed by Dr. Somorjai[38] may indeed overcome this deficiency, but the hypothesis has yet to be tested.

2.2. Prostate

Prostate carcinoma is the most common cancer affecting men in Australia[39,40] and the United States.[41] Histologic examination is the definitive standard for diagnosis and classification of prostate neoplasms.[42−44]

The IBD/NRC undertook the first MRS study (8.5T) of prostate biopsies and analyzed the data using the SCS method. The sensitivity and specificity were 100% and 95% for distinguishing benign prostatic hyperplasia (BPH) from cancer.[45] The results from this study are shown in Table 2 as is a summary of classifiers developed to date and spectral regions used to develop the classifiers.

It was notable from examining the original prostate patient cohort database that routine hospital pathology diagnosis had been used to establish study and control groups. Crucially, no prostate intraepithelial neoplasia (PIN) or proportional volumes of each type of disease state in each tissue specimen were reported. Since the SCS method is dependent upon correct and detailed histological data being reported for the computer-based strategy to generate an accurate classifier for each disease state,[14] the possibility that two such pathological entities or variants of one may have been included in one classifier was considered. In addition, the prostate is a very complex organ with four different functional zones and with mixtures of glandular and stromal tissues present in varying quantities.

A second independent MRS study of prostate biopsies[22] addressed the issue of specimen sampling for correlation with the MRS data. The spectral analysis of biopsy specimens using serially sectioned tissues identified an error rate of 8% in the routine hospital diagnosis due to incomplete sampling of the tissue.

Typical MRS spectra (8.5T) from glandular BPH, stromal BPH, PIN, and invasive adenocarcinoma are shown in Figure 3. Also compared are the spectra from tissues with different proportions of adenocarcinoma present (5% and 50%). The spectral separation of tissue with 5% adenocarcinoma from that containing only PIN was not easy on visual inspection. Resonances from lipid, amino acids, citrate, choline, and creatine are seen in the specimens containing adenocarcinoma and PIN, albeit at different levels. The BPH specimens from predominantly glandular and predominantly stromal areas are quite different, with citrate (the marker known for apparently healthy tissue) not identified in the

Table 2: Summary of Classifiers and Spectral Regions Using SCS

biopsy type (*n*)	classification	spectral regions (ppm)	accuracy (%)	ref
thyroid (107)	normal vs malignant	spectral identity not retained	99.0	61
brain (206)	control vs malignant	23/55 subregions	94.4	73
astrocytoma (91)	high vs low grade	0.81−0.85, 1.71−1.75, 2.16−2.20, 2.46−2.50, 2.54−2.58, 3.02−3.06, 3.51−3.55	95.7	191
breast FNA (140)	benign vs malignant	**1:** 0.87−0.92, 1.20−1.25, 1.63−1.67, 1.79−1.82, 1.95−1.98, 2.85−2.87, 2.95−2.97, 3.19−3.33 **2:** 1.19−1.23, 1.32−1.38, 1.79−1.82, 1.96−2.00, 2.13−2.15, 2.70−2.76, 2.92−2.94, 2.97−2.99	96.1	23
	lymph node involvement	**1:** 0.43−0.51, 0.64−0.77, 1.10−1.20, 1.56−1.59 **2:** 0.44−0.51, 0.67−0.71, 1.13−1.19, 1.56−1.60, 1.86−1.96	95.0	23
prostate (87)	benign vs malignant	3.46−3.52, 3.40−3.46, 2.50−2.56, 2.14−2.20, 1.84−1.90, 1.12−1.18	96.6	45
	residual cancer after radiotherapy	0.77−0.82, 0.94−1.00, 1.32−1.37, 1.59−1.71, 2.24−2.27, 3.19−3.28	91.4	192
liver (122)	normal vs HCC	1.34−1.37, 2.28−2.33, 2.83−2.85	100	24
	cirrhotic vs HCC	3.00−3.03, 3.56−3.60, 3.66−3.68	98.4	24
	normal vs cirrhotic	1.52−1.57, 2.03−2.08, 3.63−3.67	92.1	24
ovary (56)	normal vs cancer	1.47, 1.68, 2.80, 2.97, 3.17, 3.34	98	104
esophagus (105)	normal vs cancer	3.49−3.57, 3.23−3.28, 0.92−1.12	100	193
	normal vs Barrett's	3.50−3.54,1.93−2.06, 1.37−1.43	100	193
	Barrett's vs cancer	3.05−3.13, 2.51−2.57, 1.45−1.49, 1.21−1.29	98.6	193
melanoma	metastatic vs benign	not yet available		194
In Vivo at 1.5 T				
brain	gray vs white matter	not yet available	98	unpublished
brain	pain vs no pain	0.72−1.44, 1.64−1.83, 2.39−2.84, 3.00−3.12, 3.17−3.42	96	195
soft tissue sarcoma	normal mesenchymal vs soft tissue sarcoma		93	196

spectrum from stromal BPH. Typical spectra from stromal and glandular BPH are also shown in Figure 3 and compared with those from PIN and adenocarcinoma (see Table 1 for the assignments). It can be seen that there is a gradation in the spectra from benign stromal and glandular BPH through PIN to frankly malignant tissue with increasing volumes of tumor.

Van der Graaf *et al*. focused their study on the identification of spermine as a marker for malignancy in prostate tissue.[46] This was shown to be the case at 600 MHz on biopsy specimens, but at 1.5T it was part of the composite choline creatine resonance.

The Swindle study[22] then divided the specimens into BPH from patients with and without cancer elsewhere in the prostate, and these were both compared with adenocarcinoma specimens (Table 3).

Histologically confirmed carcinomas were determined by MR spectroscopy on the same tissue sample with a sensitivity of 100% and a specificity of 94%, but the accuracy decreased rapidly when routine hospital histology reports were used for correlation.

Depleted citrate and elevated choline levels alone were not accurate markers of malignancy, since citrate levels remain high when a small amount of malignant disease is present. It can be seen that citrate resonances are present in the spectrum from a piece of tissue containing 95% BPH and 5% adenocarcinoma (Figure 3). A recently developed mathematical regression method[38] allows small volumes of carcinoma to be identified with accuracies approaching 100% for the prostate cohort.

Although histological examination remains the standard in the assessment and examination of human prostate disease, the ability of MRS to aid in the characterization of prostate lesions on the basis of their biochemical composition may now provide additional diagnostic and prognostic information as an adjunct. MR spectroscopic databases of over 400 cases (Bourne, R., Katelaris, P., Fairy, S., Danieletto, S., Lean, C., Somorjai, R., Mountford, C., unpublished data) with detailed histology (including tumor volume and a listing of all pathological states and tissue types present) are currently being analyzed with SCS.

Cheng and colleagues, this time using quantitative histopathology and high-resolution magic angle spinning (MAS) ^{1}H MRS at 9.4T (400 MHz), undertook a study of human prostate specimens.[47] They demonstrated a linear correlation between the MRS-measured concentration of spermine, a proposed endogenous inhibitor to prostate cancer growth, and the volume percentage of normal prostatic epithelial cells as quantified by histopathology. These results indicate that MRS could serve as a means for investigating the inhibitory mechanism of spermine in human subjects.[47]

The results from the prostate programs contribute to the interesting debate as to whether there needs to be visual analysis of the MRS data if the SCS method is to be used. In the case of the prostate, if the visual analysis had not been undertaken and routine hospital histopathology had been used, the classifiers would have been developed with incorrect histopathological data. It was visual inspection of the data that identified the biopsies containing smaller volumes of cancer. However, new mathematical regression methods developed by Somorjai can identify these small volumes of cancer and offer the additional advantage that the presence of outliers can be detected. It is possible, therefore, that in the future there will be no need for simultaneous visual inspection of the data.

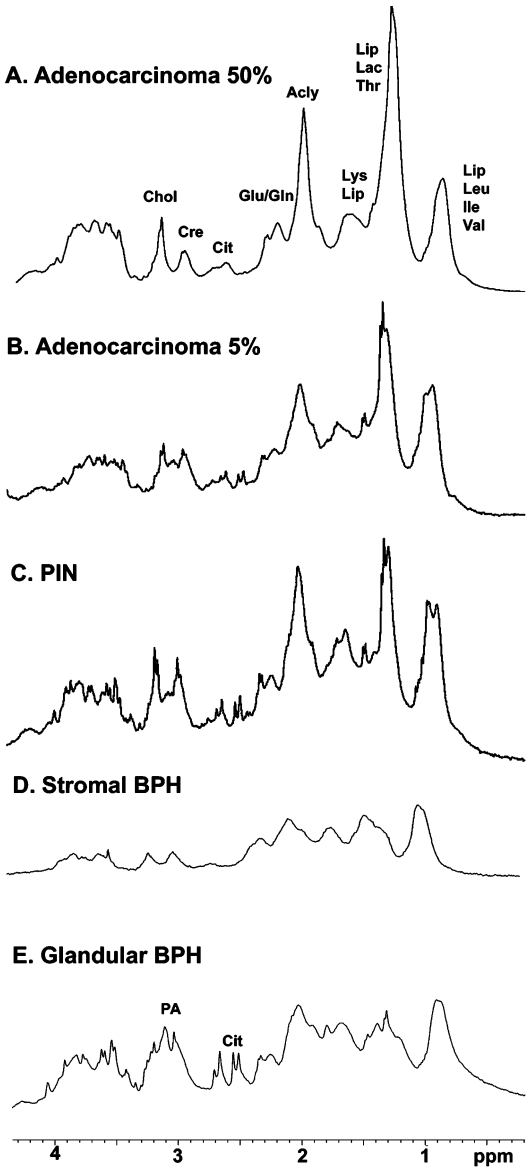

Figure 3. [1]H MR (8.5T, 37 °C) spectra of prostate biopsy specimens, 256 accumulations, sweep width 3597 Hz, pulse repetition time 2.14 s. The water peak was suppressed by selective gated irradiation. (A) Adenocarcinoma (50% of the tissue was made up of malignant tissue), (B) adenocarcinoma (5% of the tissue was made up of malignant tissue), (C) PIN, (D) stromal BPH (95% stromal, 5% glandular), and (E) glandular BPH (85% glandular, 15% stromal) are compared. Reprinted with permission from ref 22. Copyright 2003 Radiological Society of North America.

2.3. Breast

Breast cancer is the most common cancer to affect women in Western countries with an incidence of about 80−100 newly diagnosed patients per 100 000 inhabitants per year.[48] In Australia, its incidence outranks that of all other cancers in women older than 35 years and is second only to melanocytic skin cancers, which are rarely lethal. By age 75 years one in eleven Australian women will develop breast cancer.

Recent improvement in the outcome of patients with breast cancer is partly due to earlier diagnosis from screening programs and partly to more sophisticated management protocols.[49,50] The combination of physical examination, mammography, and fine-needle aspirate cytology or needle core biopsy (triple assessment) is currently the preferred method for the preoperative diagnosis of clinically or radiographically detected breast lesions. Although triple assessment has a high probability of detecting all malignant lesions, its suboptimal specificity results in diagnostic uncertainty, requiring open biopsy to exclude malignancy in many women.

In a study of 218 fine needle aspiration biopsy (FNAB) specimens from 191 consecutive patients undergoing diagnostic biopsy or definitive treatment (i.e., lumpectomy, quadrantectomy, or mastectomy) for histologically proven invasive breast cancer, [1]H MRS identified invasive carcinoma ($n = 106$) on the basis of the intensity of the 3.25 ppm resonance (choline-containing metabolites) standardized to the resonance intensity at 3.05 ppm, which contained contributions from creatine, phosphocreatine, and lysine ($P < 0.0001$, Mann−Whitney test).[21] MRS of FNAB specimens correlated with the final histological diagnosis for 96% of benign lesions. The 4% false positive rate compares with the rate of other modalities. They were, however, from four young women with fibroadenoma. The MRS of FNAB specimens correlated with a malignant histological diagnosis in 95% of the cases. These results are consistent with the reports by Aboagye and Bhujwalla and Katz-Brull,[51,52] who demonstrated, using cell models, that with malignant transformation the phospholipid metabolites alter, GPC levels decrease, and PC levels increase in the MR spectrum.

One of the most revealing studies into the diagnostic power of [1]H MRS analyzed by the SCS method is the recent study of FNAB from breast tumors. The quality of spectra obtained from these specimens can be seen in Figure 4[23], and the assignments are given in Table 1. Visual inspection of these spectra, where the choline-to-creatine ratio was measured, gave an accuracy of 95% for determining biological status. Using the SCS method, the distinction between benign and malignant biopsy specimens gave a sensitivity of 94% and specificity of 98% with an overall accuracy of 96% (Table 2). Interestingly, fibroadenoma ceased to be a false positive when the

Table 3: Comparison of Histological Examination and Accuracy[22]

malignant vs benign	type of histology	sensitivity (%)	specificity (%)
BPH from non-cancer-bearing patients	serial sectioned: adjacent piece of tissue only	100	94
including BPH from patients with cancer elsewhere in the prostate	serial sectioned: adjacent piece of tissue only	97	88
including BPH from patients with cancer elsewhere in the prostate	routine	100	82

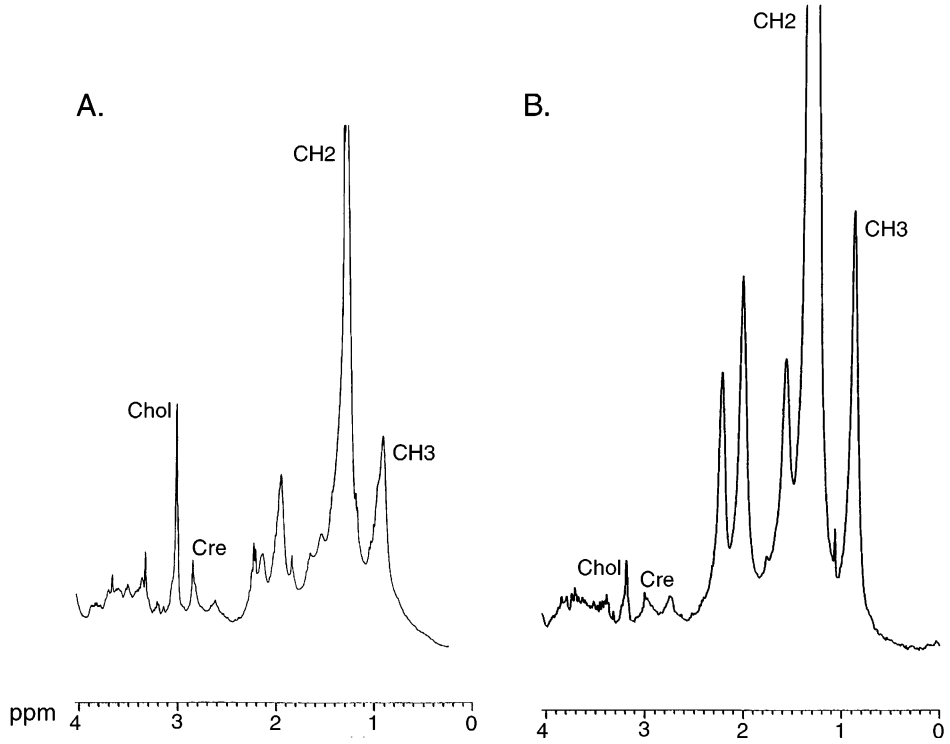

Figure 4. ^{1}H MR spectra (8.5T, 37 °C) of breast FNABs with SNR > 10: (A) malignant; (B) benign. The spectra were acquired over a sweep width of 3597 Hz, 8192 data points, 256 accumulations, relaxation delay 2 s. Reprinted with permission from ref 23. Copyright 2003 John Wiley & Sons, Ltd. on behalf of the British Journal of Surgery Society Ltd.

SCS method was implemented to analyze the MRS data.

However, from the same spectra obtained from tissue in the primary tumor and using the SCS method, lymph node involvement could also be predicted with an overall accuracy of 95%. Similarly, from the same spectrum from the primary tumor, vascular invasion in the definitive surgical specimen was predicted with an overall accuracy of 94%.[23] This is the first clinical report of information on the invasive and metastatic status of a tumor being available by inspection of a cell sample of the primary tumor. This study confirmed the initial observation made using the mouse model in 1978 that ^{1}H MRS identified cells with the capacity to metastasize. Thus, the application of MRS to the examination of FNAB from the breast has the potential to revolutionize breast cancer management by providing both diagnosis and staging parameters prior to surgery.

It will be repeated many times in this review that the entire tissue specimen needs to be examined histologically at section intervals as small as 100 μm for accurate correlation with MRS data.[53] A good example of this is breast ductal carcinoma *in situ* (DCIS), which is part of the histological continuum of epithelial cells changing from premalignant cells to fully transformed malignant cells capable of invasion and metastatic tumor formation. Examining tissue sections taken at 100 μm intervals enables the optimal assessment of the process, including the identification of features diagnostic of tissue invasion, which can be present in one field and absent in another. Such differences that may exist between two adjacent tissue sections 100 μm apart are shown in Figure 5. The top section shows lobular involvement by DCIS with a microinvasive component (confirmed by immunostaining for smooth muscle action). The bottom section, however, which was obtained 100 μm from the top section, shows no such evidence of invasion, and the H + E appearances in these two sections are virtually indistinguishable. The MR spectra consistent with these two diagnoses are shown alongside and are clearly different.

Visual inspection of the MR spectra demonstrated that cases where DCIS had breached the basement membrane (<1 mm) in one or more foci (i.e., microinvasion) and those with extensive comedonecrosis had spectra similar to those of frankly malignant lesions.[21] Other cases of DCIS, without microinvasion, contained far less chemical activity and were more readily correlated with benign specimens (Figure 5). As yet, insufficient data have been accumulated on the DCIS category for an SCS classifier to be developed.[53] However, as can be seen in the case studies (section 5), the application of MRS to biopsies of the breast, used in conjunction with MRI, can provide important clinical information. It may be that high-grade DCIS (i.e., of comedocarcinoma type) already has the biochemical machinery to invade and metastasize but not yet the opportunity to express it histologically (i.e., truly preinvasive carcinoma).

Sitter and colleagues used ^{1}H MAS and 2D *J*-resolved spectroscopy, again on a small patient cohort to provide careful resonant assignment of both breast tissue specimens and extracts.[54]

Cheng studied 19 female ductal carcinomas using ^{1}H MAS MRS; alterations to cellular metabolism including the choline-related metabolites demonstrated a distinction between healthy tissue and carcinoma. This included alterations in the T_2 relax-

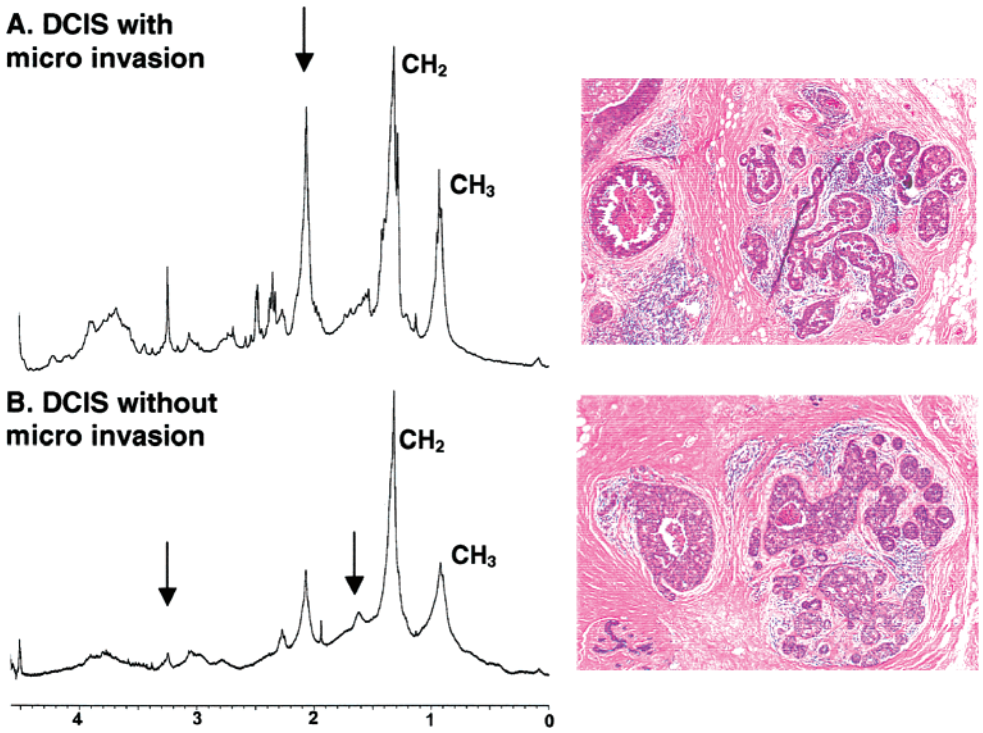

Figure 5. [1]H MR spectra (8.5T, 37 °C) of fine-needle biopsy specimens obtained from breast ductal carcinoma *in situ*: (A) with microinvasion present; (B) without microinvasion. Histology slides of tissue containing DCIS are shown in (A) with microinvasion present and (B) without microinvasion. The spectra were acquired over a sweep width of 3597 Hz, 8192 data points, 256 accumulations, relaxation delay 2 s. Reprinted with permission from ref 53. Copyright 2000 Lippincott Williams & Wilkins.

ation time of cellular metabolites in the cancerous tissue. Of particular interest was the finding that tumor metabolic markers including phosphocholine, lactate, and lipids correlated with the histopathological grade.[55] This was an important observation, and verification using larger databases can now be examined retrospectively.

2.4. Liver

A common internal malignancy worldwide is primary hepatocellular carcinoma (HCC).[56] In 1998 it was the most frequent tumor in males[57] and the most common in Asia and Africa. The annual incidence in Western countries is 4 per 100 000.[57] HCC almost always occurs as a sequel to cirrhosis and is increasingly prevalent because of the upsurge in cases of chronic hepatitis B and hepatitis C.

Biopsies obtained from apparently normal liver, cirrhotic liver, and HCC were examined by [1]H MRS at 8.5T. The correlative histopathology from 54 consecutive patients undergoing hemihepatectomy or total hepatectomy was obtained from Royal Prince Alfred Hospital[24] in Sydney, where the Australian National Liver Transplant Unit is located.

Typical MR spectra from HCC, cirrhotic, and apparently healthy liver are compared in Figure 6. In this case resonance assignments were made from 2D [1]H−[1]H COSY (Figure 7) and were confirmed by [1]H−[13]C HSQC (not shown). The assignments are summarized in Tables 1 and 4.[24] In these studies, SCS-based classification of [1]H MR data from the liver biopsies distinguishes normal liver from HCC with

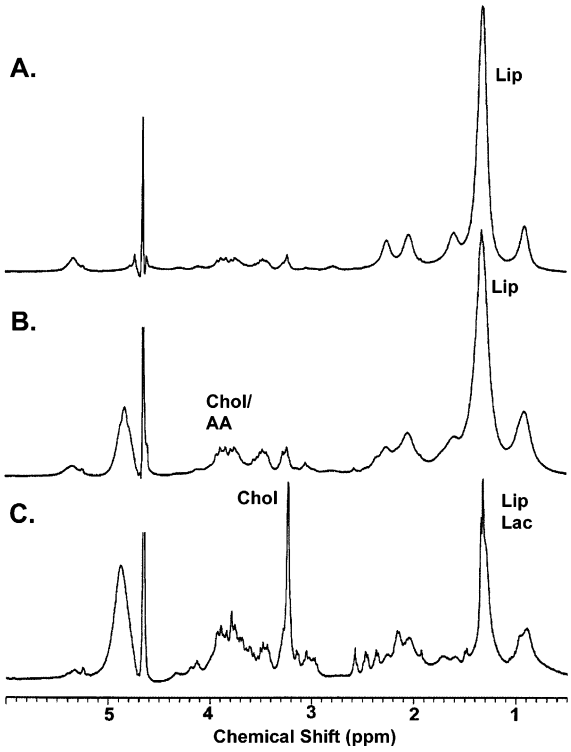

Figure 6. [1]H MR spectra (8.5T, 37 °C) of liver biopsy specimens: (A) normal liver; (B) cirrhotic liver; (C) HCC. The spectra were acquired with water suppression using selective gated irradiation, sweep width 3600 Hz, 8K data points, 256 accumulations, repetition time 2.3 s. Reprinted with permission from ref 24. Copyright 2002 Taylor and Francis (http://www.tandf.co.uk/journals/titles/00313025.html).

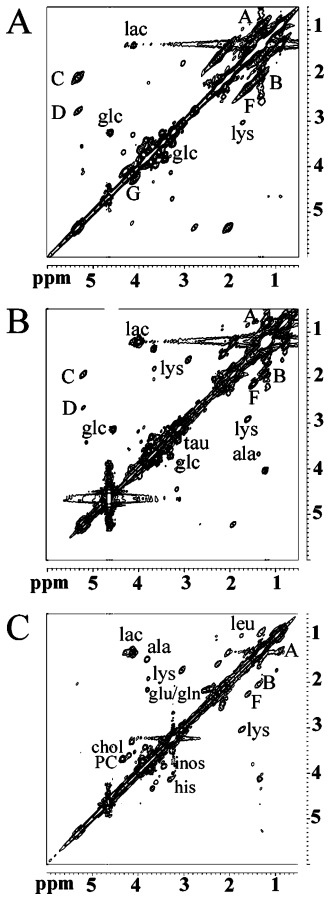

Figure 7. Typical 2D $^1H-^1H$ COSY spectra from biopsy samples of (A) normal liver, (B) chirrotic liver, and (C) HCC, 48 accumulations, 200 experiments. The spectra were processed using a sine-bell, Lorentzian−Gaussian (LB = −30, GB = 0.20) window function, in the t_1 and t_2 domains, respectively. Reprinted with permission from ref 24. Copyright 2002 Taylor and Francis (http://www.tandf.co.uk/journals/titles/00313025.html).

100% accuracy. The SCS method also distinguishes cirrhotic liver from HCC with an accuracy of 98.4%. The distinction between normal and cirrhotic liver is, however, less accurate at 92%.

The clinical end point of these studies is to allow discrimination between HCC and its "tumor look-alikes"; this can be very difficult in small biopsies, but is less of a problem in partial or complete hepatectomy specimens where test sample selection can be controlled. To guarantee the integrity of the SCS data, further studies are required using selected tissues from only those cases where the histopathologist can guarantee the diagnosis (i.e., "classic cases") and excluding those cases, or biopsies from areas, in which there is uncertainty about the histological diagnosis. From such studies, it is hoped that firm discriminatory criteria will be identified, which will supplement histological assessment in difficult cases.

It now remains to be seen if this technology can be extended to the *in vivo* situation where it would provide clinically significant preoperative information. Nevertheless, the SCS analysis of MRS offers a new and accurate supplementary means for the objective diagnosis of HCC.

Table 4: Assignment of Resonances in ^1H MR COSY Spectra

			chemical shift (ppm)	
molecule	abbrev	species	F_2	F_1
		Lipids		
triglyceride[a]	A	$(CH_2)_nC\mathbf{H}_2C\mathbf{H}_3$	0.90	1.33
	B	$=CHC\mathbf{H}_2C\mathbf{H}_2-$	1.33	2.08
	C	$CH=C\mathbf{H}$-$C\mathbf{H}_2$	2.02	5.38
	D	$CH_2C\mathbf{H}$-CH	2.84	5.38
	E	$C\mathbf{H}_2C\mathbf{H}_2$	1.33	1.62
	F	$O=CC\mathbf{H}_2C\mathbf{H}_2$	1.60	2.30
	G	$OC\mathbf{H}_2C\mathbf{H}O$	4.12	5.26
			4.26	5.26
	G	$OC\mathbf{H}_2$	4.09	4.29
		Amines		
choline	Chol	$NC\mathbf{H}_2C\mathbf{H}_2$	3.50	4.07
phosphorylcholine	PC	$NC\mathbf{H}_2C\mathbf{H}_2OP$	3.61	4.25
glycero-PC	GPC	$NC\mathbf{H}_2C\mathbf{H}_2OPO$	3.69	4.38
		Amino Acids		
alanine	Ala	$C\mathbf{H}C\mathbf{H}_3$	1.49	3.79
histidine	His	$C\mathbf{H}C\mathbf{H}_2$-ring	3.22	3.95
leucine	Leu	$C\mathbf{H}C\mathbf{H}_3$	0.97	1.78
lysine[b]	Lys	$C\mathbf{H}_2C\mathbf{H}_2$	1.72	3.05
threonine	Thr	$HOC\mathbf{H}C\mathbf{H}_3$	1.33	4.27
valine	Val	$C\mathbf{H}C\mathbf{H}_3$	1.03	2.34
		Other		
taurine	Tau	$H_2NC\mathbf{H}_2C\mathbf{H}_2OS$	3.28	3.50
lactate anion	Lac	$C\mathbf{H}C\mathbf{H}_3$	1.33	4.12
fucose	Fucl	$C\mathbf{H}C\mathbf{H}_3$	1.33	4.27
unassigned			0.90	1.50
			1.20	3.65
			1.30	4.65
			1.50	1.95
			1.95	3.80
			2.10	2.40
			2.20	2.40
			2.65	2.85
			3.15	3.35
			3.60	3.90

[a] Cross-peaks A−F from fatty acyl chains and G and G′ from the glycerol backbone. [b] And polyamines.

2.5. Thyroid

Thyroid cancer is rare, but many thyroidectomies are performed simply to exclude malignancy. On the other hand, thyroid nodules are common. The vast majority (90−95%) of solitary thyroid nodules are benign.[58−60] The exclusion of follicular thyroid malignancy remains a significant diagnostic problem, currently made on biopsy material obtained following a thyroidectomy. That means some people have their entire thyroid removed essentially for diagnostic purposes. Ninety-five percent of such people prove to have genuinely benign thyroid disease. Preoperative FNAB cytology, although accurate in identifying papillary, medullary, and anaplastic carcinomas, is unable to reliably distinguish benign from malignant follicular neoplasms.

Histologically, tumors that are arbitrarily designated as follicular adenomas and follicular carcinomas are indistinguishable on the basis of clinical, radiological, and gross pathologic features and rely on the identification of capsular or vascular invasion at the edge of the lesion to confirm malignancy. The extreme difficulty facing the clinicians selecting potential malignant thyroid nodules for surgery was

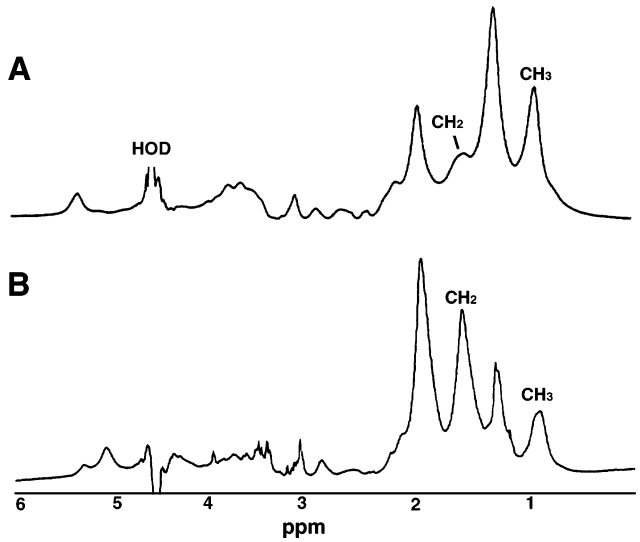

Figure 8. [1]H MR (8.5T, 37 °C) spectra from (A) follicular carcinoma and (B) benign follicular adenoma. The spectra were acquired with 256 accumulations, and residual water was suppressed using gated irradiation. Diagnostic resonances at 0.9 ppm (CH_3, lipid) and 1.7 ppm (CH_2, lysine) are denoted. $+N(CH_3)_3$ = *N*-trimethyl from choline-containing metabolites; HOD = residual water. Reprinted with permission from ref 81. Copyright 1997 Elsevier.

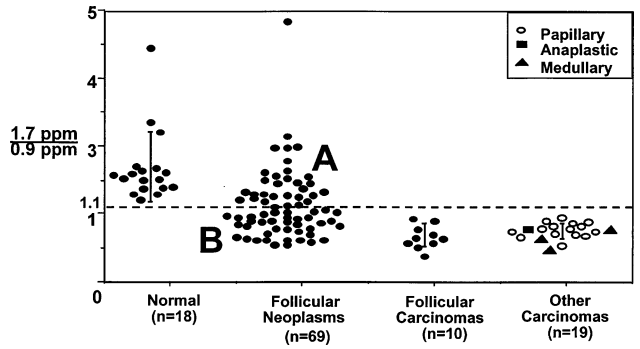

Figure 9. Ratio of resonances at 1.7 and 0.9 ppm for normal thyroid tissue, follicular neoplasms, and malignant thyroid biopsies. Histologically proven follicular cancers all have a ratio below 1.1, whereas "non-malignant" follicular neoplasms fall into groups, comparable with either normal or carcinomatous tissue. A separation of ratios above and below 1.1 is observed with no overlap between normal and malignant tissue. Reprinted with permission from ref 34. Copyright 1994 Springer-Verlag.

the subject of an editorial by Ernest L Mazzaferri in the *American Journal of Medicine*.[60]

In the first MRS study, tissue was obtained intraoperatively (at the time of surgery) from 53 consecutive patients undergoing partial or total thyroidectomy for solitary thyroid nodules.[19] Typical [1]H MR spectra (8.5T) of follicular adenoma and follicular carcinoma are compared in Figure 8. On visual inspection, and by measuring the ratio of resonances at 1.7 and 0.9 ppm, MRS was able to distinguish normal tissue from carcinomas (proven clinically or histologically) with an accuracy of 100%.[19] When this resonance ratio was measured for histologically similar follicular adenomas, some specimens were found to be spectrally grouped with the benign lesions and others with the carcinomas (Figure 9). The most tempting explanation is that the adenomas with a "malignant" spectral pattern were, indeed, noninvasive or preinvasive follicular carcinomas (i.e., in the process of transformation). These thyroid data were used for the first application of the SCS method to human biopsy.[61] An accuracy of 100% was reported for normal thyroid vs carcinoma. The same information and diagnostic accuracies obtained for visual inspection of thyroid tissues can also be obtained from FNAB of the thyroid obtained intraoperatively.[36]

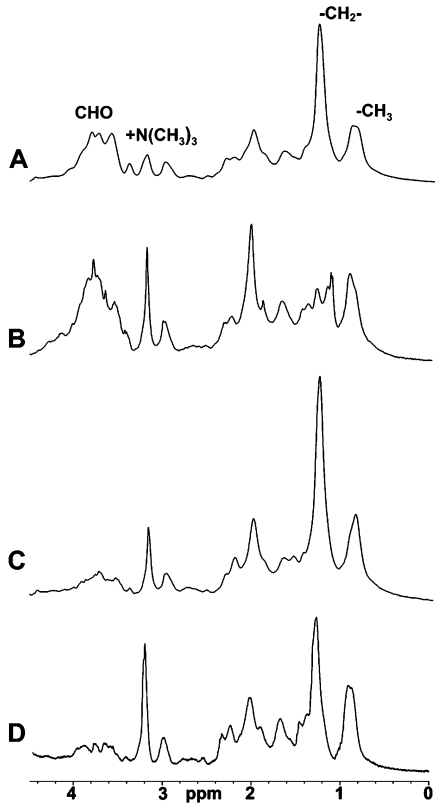

Figure 10. [1]H MR (8.5T, 37 °C) spectra of esophageal biopsies from 4 different histopathological subtypes: (A) normal esophagus; (B) Barrett's epithelium from non-cancer-bearing patients; (C) Barrett's epithelium from cancer-bearing patients; (D) adenocarcinoma. The spectra were acquired with 256 accumulations, and residual water was suppressed using selective gated irradiation, sweep width 3600 Hz, 8K data points. Reprinted with permission from ref 193. Copyright 2003 Excerpta Medica Inc.

The specimens used for the above MRS analysis were obtained intraoperatively, i.e., when there was no blood supply to the thyroid. To make this MRS method applicable to the clinical situation, FNABs were taken from the thyroid, preoperatively, and thus with normal blood supply. The thyroid is a very vascular organ, and the FNAB contained a significant amount of blood, which was found to mask the diagnostic chemical signature (Mackinnon, W.; Lean, C.; Russell, P.; Delbridge, L.; Malycha, P.; Mountford, C., unpublished data). It has yet to be determined if the MRS data containing varying levels of blood can be analyzed by the SCS method. Thus, for the MR method to assist in the management of patients with thyroid cancer, an *in vivo* MRS methodology needs to be developed (see section 5).

2.6. Esophagus

Adenocarcinoma of the lower esophagus in the Western world is rising and accounts for more than

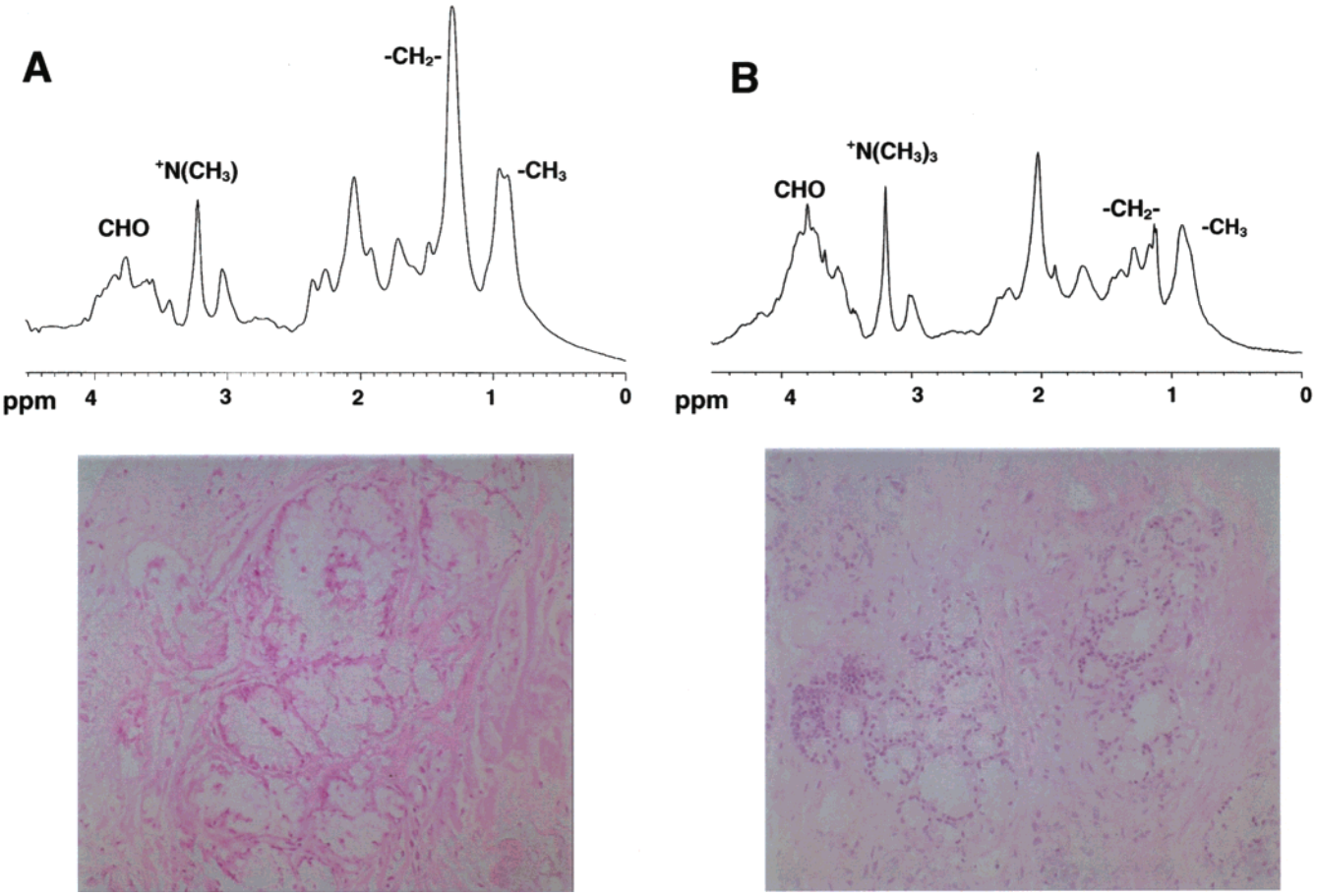

Figure 11. ^{1}H MR (8.5T, 37 °C) spectra of Barrett's epithelium from (A) cancer-bearing patients and (B) non-cancer-bearing patients with the corresponding histopathology. The staining method was hematoxylin and eosin, magnification ×200. The spectra were acquired with 256 accumulations, and residual water was suppressed using selective gated irradiation, sweep width 3600 Hz, 8K data points. Reprinted with permission from ref 193. Copyright 2003 Excerpta Medica Inc.

40% of esophageal carcinomas in males.[62] The condition is thought to result from gastric reflux, and so-called Barrett's esophagus is a precursor,[63] which increases the risk of developing malignancy 40−50-fold.

Histopathology can accurately distinguish normal from invasive carcinoma in the esophagus. The accurate prediction of the behavior of dysplastic Barrett's epithelium is, however, not possible.[64,65] MRS was considered as a possible objective technique to identify Barrett's patients at risk of progressing to adenocarcinoma; i.e., could the MRS method identify a chemical fingerprint associated with commitment to malignancy that was not morphological?

In a study investigating 72 consecutive patients, 29 non-cancer-bearing and 43 cancer-bearing, ^{1}H MRS of esophageal biopsies combined with the SCS strategy provided a robust diagnosis with a high degree of accuracy for discriminating normal epithelium from esophageal adenocarcinoma and Barrett's esophagus (Table 2). A typical 1D MR spectrum (8.5T) of normal healthy esophageal tissues is shown in Figure 10A and compared with that of adenocarcinoma of the esophagus in Figure 10D. As with the breast, a major difference is the intense choline resonance in the adenocarcinoma spectrum.[52,66]

Different spectral categories of Barrett's epithelium were identified by visual inspection (Figure 10B,C). The 1D ^{1}H MR spectra of Barrett's epithelium from a non-cancer-bearing patient and from a cancer-bearing patient with the corresponding histopathology are shown in Figure 11. Histologically, these tissues are indistinguishable, yet the MR spectra group the specimen from the cancer-bearing patient with the adenocarcinomas. There is substantial evidence supporting the existence of an adenoma−carcinoma sequence in the esophagus.[67−69] These MRS data support the MR method being able to identify a field change consistent with the presence of an adenoma−carcinoma sequence.

The esophagus MRS study has now been in progress for over 6 years. The patients are informed of the "research outcome" of the MRS analysis. A number of the patients identified as having tissue committed to malignancy during the study are now presenting for surgery in subsequent years for clinical cancer (Falk, G.; Doran, S.; Phillips, J.; Lean, C.; Russell, P.; Mountford, C., unpublished data). As with many of these clinical studies, the predictive nature of the MRS analysis must wait a considerable number of years for patient outcomes to be documented and correlated (i.e., de facto clinical trials).

2.7. Brain Tumors

Survival rates among brain tumor patients vary considerably depending on the type and grade of

neoplasm, and accurate diagnosis can significantly alter therapeutic planning, potentially improving the clinical outcome.[70−72] Diagnosis of brain tumors relies extensively on histopathological evaluation of cellular changes of open biopsy specimens. Classification of human brain tumors is often varied as a result of the complexity of tumor cell biology and discrepancies in the descriptive nature of morphology-based histopathology.

There is a relatively large body of literature on the application of MRS to brain cancers. The majority, however, have involved *in vivo* studies with the following exceptions. In a study by Somorjai *et al*. MR spectra of biopsies from subjects with meningiomas (95), astrocytoma (74), and epilepsy (37) were analyzed using the SCS method. The SCS method could reliably distinguish between various types of brain cancer[73] with accuracies approaching 100%. Tzika *et al*. undertook the biochemical examination of pediatric brain tumor biopsies following *in vivo* MRS, with a view to investigating tumor metabolism and to establish biochemical criteria crucial for detailed and precise classification of neoplasms to improve diagnostic accuracy.[74] Tzika demonstrated that neoplasms can have altered metabolism which precedes histologically observable changes to cellular morphology.[75]

Interestingly, in the study undertaken by Cheng *et al*.,[76] it was demonstrated that *ex vivo* MAS MRS provided line widths that were approaching those of *in vivo* spectroscopy at 1.5T. Analysis of the *ex vivo* spectra showed prominent inositol and glycine resonances in high-grade tumors, and the tumor-specific Cho peak that was detected *in vivo* was resolved into 3 different resonances: glycerolphosphocholine (GPCho), phosphorylcholine (Pcho), and choline (Cho). The resonance ratio of inositol (at 4.05 ppm) to creatine was effective in distinguishing tumor type, suggesting that the MAS method for intact tissue measurement could be used as an adjunct to histopathology and could improve the accuracy for brain tumor diagnoses (Figure 12).[76] Subsequent linear regression analysis (LGA) showed that the selected metabolite ratios from *in vivo* and *ex vivo* spectra were strongly correlated. The agreement between *in vivo* and *ex vivo* MRS suggests a multimodality approach could provide a link between *in vivo* MRS and neuropathological analysis.[74]

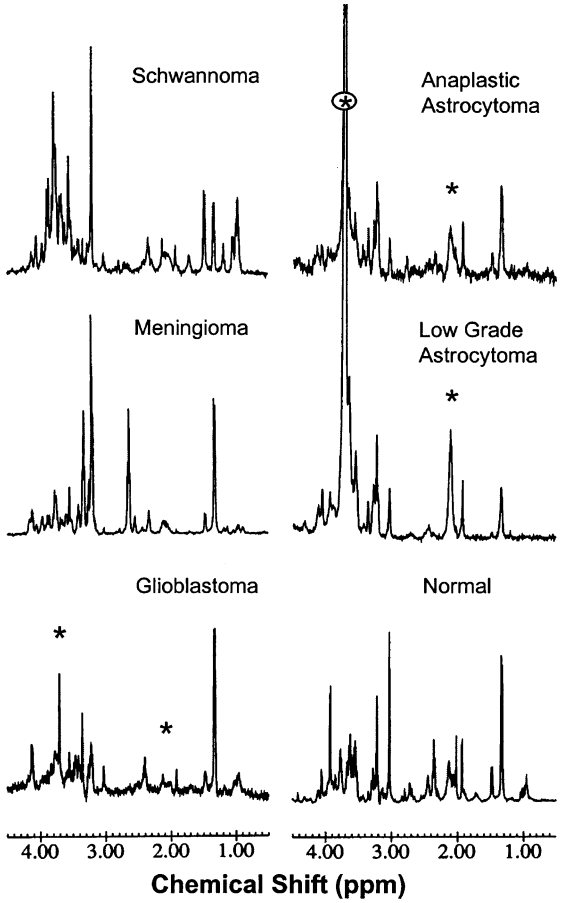

Figure 12. HR MAS ^{1}H MR spectra of intact tissue specimens from various types of human brain tumors and normal brain tissue. An asterisk indicates possible chemical contamination during pathological processing. A total of 512 accumulations were taken, with an acquisition time of 0.819 s. A repetition time of 3 s and a spectral width of 8000 Hz were used. Reprinted with permission from ref 76. Copyright 1998 American Association for Cancer Research, Inc.

2.8. Squamous Cell Carcinoma of the Head and Neck

Histopathology remains the gold standard for definitive diagnosis of squamous cell carcinoma in the head and neck, but it does require invasive procedures to obtain the biopsy. Leemans *et al*. have shown that between 15% and 30% of stage 3−4 patients with histological tumor-free resection margins have recurrence of the disease.[77] It is exactly this type of clinical dilemma where the MRS method has proven valuable in other organs.

El-Sayed and colleagues investigated the diagnostic potential of ^{1}H MRS at 8.5T to diagnose squamous cell carcinoma of the head and neck. They compared tumor and adjacent normal histological tissue specimens from untreated head and neck cancer patients.[78] The study, which included 54 specimens but taken from only 15 patients, applied the SCS method to the MRS data. Squamous cell carcinoma was distinguished from normal tissue with an accuracy of 93%. A larger study with appropriate clinical followup needs to be undertaken to establish robust classifiers for this organ. This study is also likely to form the basis of high-field *in vivo* MRS analysis to provide a noninvasive diagnosis.[78,79]

3. Adenoma–Carcinoma Sequence Identified by 2D MRS

The 2D COSY method was first applied to cells in 1984,[13] and after extensive experimentation the long T_2 resonance which identified tumors with the capacity to metastasize was assigned to cell surface fucosylated moieties.[28] 2D COSY spectroscopy demonstrated that cells and tissues can give rise to resonances from up to 60 different chemical species, all of which can alter simultaneously (Table 4). Unlike stable chemical compounds and relatively stable proteins for which 2D spectroscopy was designed, biopsy specimens and tissues *in vivo* generate

extremely busy spectra. There is a finite time during which the data can be collected, and each tissue type must be considered independently when 2D data are acquired, inspected, and analyzed. It must also be considered that suspensions of cells will have a lower than physiological pH, and some pH-dependent molecules will thus have altered chemical shifts. Tissue specimens tend not to undergo such a significant alteration in pH.

The appearance and interpretation of 2D data of biological and human material depend on the protocol for data collection and processing. Relative cross-peak intensities can change dramatically depending on the choice of window function maxima. It is not uncommon for the same data file to be processed in three or four different ways for the wide range of T_2 species to be compared and contrasted.[28,80] It is this detailed and complex interrelationship of biochemical pathways that provides the diagnostic and prognostic information.[28−30,81,82] The SCS method has not yet been developed for 2D data analysis.

3.1. Colorectal Cells

The rationale that MRS could aid in the pathological assessment of colorectal cancer was proposed in a study of human biopsies.[83−86] Spectral differences were reported which broadly correlated with clinical staging of the disease by current methods of pathological assessment. MRS studies on cell lines were undertaken to better understand the chemical differences associated with the adenoma−carcinoma sequence in developing colorectal cancers.

Human cultured colorectal cell lines with known growth characteristics, degree of differentiation, tumorigenicity, and metastatic potential became available for study in the 1970s.[87−95] The cell lines allowed colorectal tumor development and progression in vitro to be studied in a defined reproducible manner in the laboratory.

Initially, two human malignant colorectal cell lines, LIM1215 and LIM1863, were chosen for study on the basis of their different tumorigenicity. Both cell lines were epithelial in type and contained two of the three major types of cells found in mature colon, columnar and goblet. A typical 2D COSY spectrum from the highly tumorigenic cell line LIM1215 is shown in Figure 13A and compared with that of the lowly tumorigenic cell line LIM1863 (Figure 13B). Dominant lipid cross-peaks denoted A−G′ in Figure 13 were assigned to triglyceride. Other cross-peaks from choline, phosphorylcholine, glycerophosphorylcholine, inositol, taurine, lactate, free amino acids, and peptides were also assigned[96] and with other resonances are summarized in Table 4.

Using these cell lines, the origins of the long T_2 resonances that were diagnostic for tumor dissemination were assigned by Lean and colleagues[28] and the assignments confirmed by Listinsky *et al.*[97] (unpublished data). The H5, H6 cross-peaks for fucosyl residues lie in the region of the COSY spectrum corresponding to $-CH(OH)CH_3$ moieties with coordinates 3.9−4.5 and 1.0−1.6 ppm. This region also contains cross-peaks from lactate and threonine (Table 4). The precise origin and biological

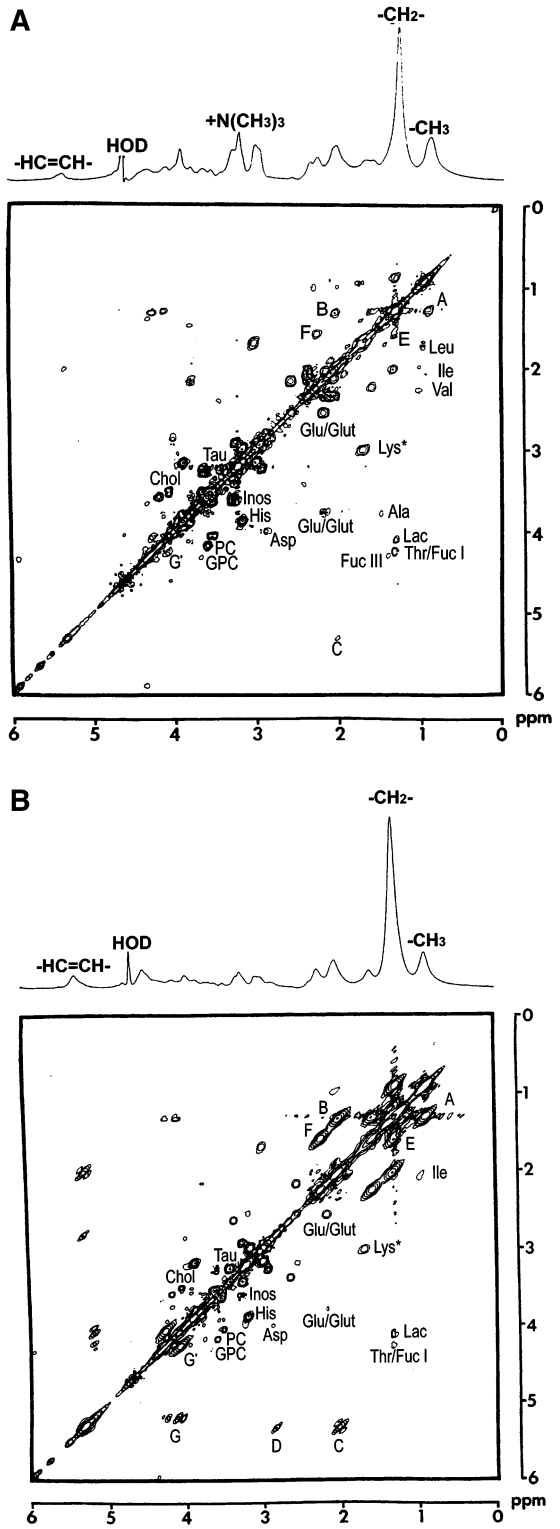

Figure 13. ^{1}H (8.5T, 37 °C) MR, 1D (100 scans) and symmetrized COSY (32 scans, 220 FIDs), spectra of 10^8 subconfluent (A) LIM1215 (highly tumorigenic) and (B) LIM1863 (lowly tumorigenic) malignant colorectal cells in 400 μL of phosphate-buffered saline in D_2O. The data were obtained at 37 °C with the sample spinning. A line broadening of 3 Hz was applied to the 1D MR spectrum, and sine-bell and Lorentzian−Gaussian (LB = −30.0, GB = 0.20) window functions were used in the t_1 and t_2 domains, respectively, for the COSY spectrum. Contour plots were generated with the lowest level set close to the noise level and subsequent levels increasing in powers of 2. Reprinted from ref 28. Copyright 1992 American Chemical Society.

role of these cell surface fucosylated species were further studied using an extended cell model where cultured human colorectal cell lines with known growth characteristics and varying degrees of differentiation, tumorigenicity, metastatic potential, and genetic abnormalities made it possible to simulate colorectal tumor development and progression in vitro.[88,98−100] 2D COSY spectra were obtained for each of the six cell lines. Cross-peaks for the following were assigned (Table 4): the lipid metabolites choline, phosphocholine, phosphoethanolamine, and glycerophosphocholine;[96] the amino acids alanine, aspartate, glutamate, glutamine, leucine, lysine, proline, threonine, and valine;[101] other molecules including myoinositol, taurine, fucosyl residues,[28,102] and the ribose and glycosamine moieties of uridine diphospho-*N*-acetylglucosamine (UDP-ClcNAc) (not shown).

With increasing tumorigenicity there was a striking correlation with the increased ribose H1′ and H2′ protons of UDP-hexose (5.99 and 4.38 ppm). Similar trends were observed in the ratio of ribose to lysine and ribose to choline. In both cases, the ratio increased abruptly in the highly tumorigenic lines, and these tailed off. The ribose-to-fucose ratio trend was almost identical to that of ribose to choline, indicating a larger relative volume increase in UDP-hexose than occurred in bound fucose.

Expansion of the spectra in the regions 3.9−4.5 and 1.0−1.6 ppm (−$CH(OH)CH_3$ moieties) from the six colorectal cell lines are shown in Figure 14. The total volume of the cross-peaks labeled Thr/Fuc I and Fuc II, IIb, and III was measured, and ratios with the same reference cross-peak volumes used above were calculated. An increase from adenoma to carcinoma was observed most clearly for the fucose-to-valine cross-peak ratio.[29]

Reports by Hakamori and colleagues strongly suggested that these fucose lipids were characteristic of the Le^y antigen of human adenocarcinoma as trifucosylnonaosyl Le^y glycolipid (III^{3}FucV^{3}FucVI^2-FucnLc$_6$).[103] Interestingly, this spectral region was one of those selected by the SCS method to identify cells in the primary breast tumor capable of disseminating to the lymph nodes.[23] These results were substantiated by correlating the ^{1}H MRS analysis of human colorectal biopsies with histopathology.[18]

3.2. Ovary

In the early stages of developing the SCS method, more basic multivariate techniques were employed. In particular linear discriminant analysis (LDA) was used to distinguish normal ovarian tissue from ovarian cancer with a sensitivity of 100% and a specificity of 96% (an accuracy of 98%, Wallace *et al.*). Moreover, LDA was able to distinguish untreated ovarian cancer from recurrent ovarian cancer with a sensitivity of 92% and a specificity of 100% (accuracy of 97%). Removal of one ("fuzzy") specimen that was unable to be classified with a probability greater than 75% increased the accuracy to 100%.[104]

Ovarian cancer was thought to have an adenoma−carcinoma sequence, but it remained undefined. Two dimensional COSY analysis provided a unique insight into the presence of the adenoma−carcinoma

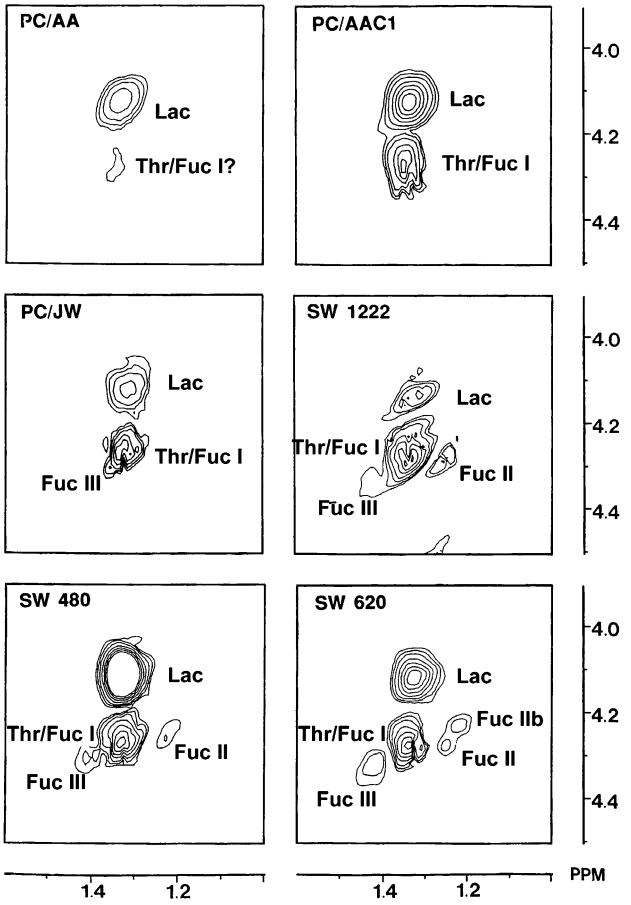

Figure 14. Expansions of the −$CH(OH)CH_3$ region (F_2, 1.00−1.60 ppm; F_1, 3.90−4.50 ppm) from the ^{1}H MR (8.5T) symmetrized COSY data from colorectal cells grown in vitro: PC/AA, PC/AAC1, PC/JW, SW 1222, SW 480, SW 620, in order of decreased cellular differentiation. The absolute-intensity contour plots were generated with the lowest level (500) (set close to the noise level); for levels 2 and 3 the increment was 250 and for subsequent levels 500. Reprinted with permission from ref 15. Copyright 1993 Academic Press.

sequence in ovarian cancer. The traditional histological subdivisions of benign, proliferating, and malignant ovarian tumors are according to strict morphological criteria. However, ovarian surface epithelial/stromal neoplasms are a group of related yet different entities. The position of the proliferating tumors is a clinical question that needed addressing,[105−107] and not all proliferating tumors are considered part of this sequence.

The distinction between benign neoplasms or normal tissue on one hand and carcinoma on the other hand was made from 1D MR spectra by comparing the resonance intensities of creatine/phosphocreatine and lysine, providing a sensitivity and specificity of 87% and 97%, respectively.[16] The low sensitivity was due to inappropriate sample-handling procedures. Proliferating tumors exhibited a range of 1D spectral patterns. Cell-surface fucose was altered with tumor development and progression. The increasing complexity of the COSY fucosylation spectral pattern with tumor development and progression is illustrated in Figures 15 and 16. In Figure 16 the COSY spectrum of normal ovary is shown expanded (F_1, 3.9−4.5 ppm; F_2, 1.0−1.6 ppm) and compared to that

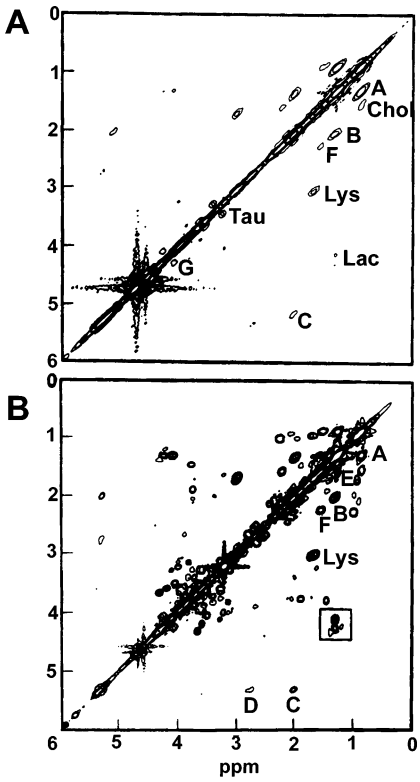

Figure 15. ^{1}H MR magnitude-mode COSY spectra of (A) normal ovarian tissue and (B) poorly differentiated serous carcinoma, 64 accumulations, 200 experiments. The spectra were processed using a sine-bell, Lorentzian−Gaussian (LB = −40, GB = 0.12) window function, in the t_1 and t_2 domains, respectively. Key: A−F, from fatty acyl chains; G′, from gerimal protons on the glycerol backbone of triglycerides; Chol, cholesterol; Lys, lysine; Lac, lactate. Reprinted with permission from ref 16. Copyright 1995 Blackwell Publishing.

from benign and proliferating serous tumors and carcinomas of increasing histologic grade. The cross-peaks detected in this region are recorded in Table 4, from which it can be seen that multiple resonances from cell-surface-bound fucose generally characterized the carcinoma specimens and many (but not all) of the proliferating tumors. Using these criteria, namely, the additional presence of Fuc II, IIb, or III vs Thr/Fuc I alone, serous, mucinous, endometroid, and mixed epithelial carcinomas were distinguished from benign/normal tissue with a sensitivity and specificity of 88% and 97%, respectively. The multiple cross-peaks from cell-surface fucose in the COSY spectra of ovarian carcinoma were directly comparable to those reported for colorectal epithelial tumors.[15,18]

Two-dimensional MRS methods provide unequivocal assignment of resonances from chemical species that contribute to the various pathological states defined during tumor development and progression. Diagnostic resonances indicative of the capacity of a tumor to spread to other sites of the body are associated with the increasing presence of cell-surface fucosylation. Furthermore, these data provided strong evidence for the existence of an adenoma−carcinoma sequence in some tumor types in the ovary. For a review of the role of fucose and the pathological process see Listinsky *et al.*[97]

4. Proton MRS in Vivo

The clinical applications of MRS *in vivo* have improved significantly over the past decade. Single-voxel MRS and studies of magnetic resonance spectroscopic imaging (MRSI) of both brain and prostate have shown unequivocally that the method can

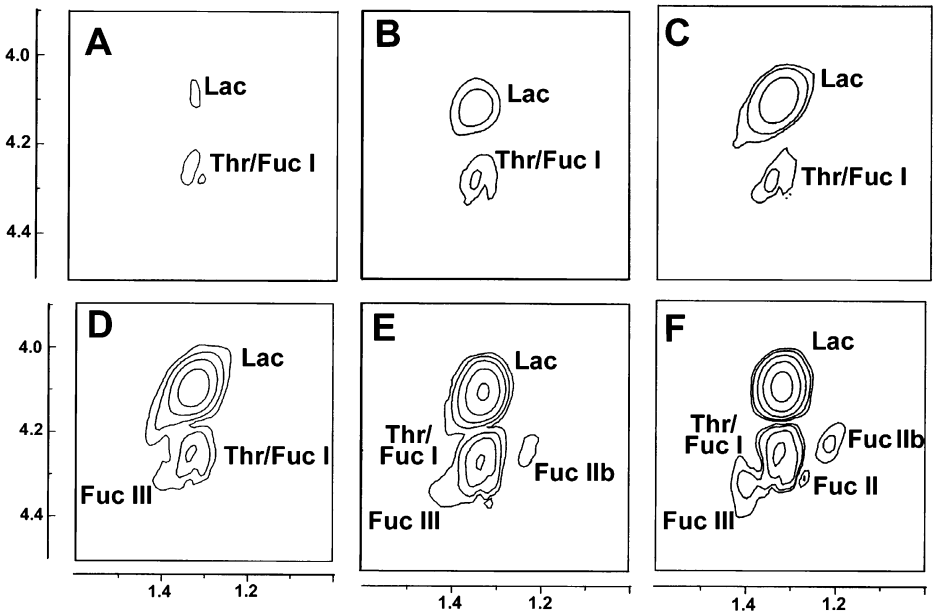

Figure 16. Expanded methyl−methine coupling region (F_1, 3.9−4.5 ppm; F_2, 1.0−1.6 ppm) from the 2D COSY spectra (Figure 15) showing increasing complexity of the fucosylation pattern with histologic grade for serous tumors. Contour levels started at 6000 and increased exponentially. Key: (a) normal ovary; (b) benign tumor; (c) proliferating tumor; (d) well-differentiated carcinoma; (e) moderately differentiated carcinoma; (f) poorly differentiated carcinoma; Thr/Fuc I, Fuc III, II, and IIb, resonances attributable to bound fucose, with a contribution from threonine to Thr/Fuc I. Reprinted with permission from ref 16. Copyright 1995 Blackwell Publishing.

identify metabolite levels which may be correlated with human disease states with reasonable accuracy. When the expensive and detailed pathological examination of biopsy material (as described in section 2 on biopsy specimens) is correlated with *in vivo* spectra, it is expected that the accuracies will be very high.

Of importance, it has now been established that by using current MRSI methodology[108] the MRI and MRS data collection can be acquired within the same clinical examination and within a time frame that is acceptable for patient management. Techniques for water suppression will not be discussed as part of this review, nor will outer volume suppression (OVS) sequences. It must be understood, however, that for chemical species to be available for inspection both issues need to be appropriately addressed.

There has been a tendency in some *in vivo* MRS applications to suppress the lipid and water to record the smaller, less intense resonances, which were likely to be informative. It must be recognized that any suppression techniques, whether they be water or lipid, will have an impact on a significant component of the rest of the spectrum and might reduce or remove altogether metabolites of interest. Interestingly, Lenkinski[109] has investigated the possibility of obtaining MR spectra *in vivo* with neither water nor lipid suppression. Thus, there is currently debate on the philosophy of outer voxel lipid suppression and unsuppressed water.

4.1. Neurospectroscopy

Neurospectroscopy is the application of MRS to the brain and currently the most widely used MRS application in the clinic. The first application of neurospectroscopy was undertaken using a surface coil,[110] and appropriate localization was developed by Bottomley.[111] However, for the clinical setting, more advanced localization techniques such as 90°−90°−90° Stimulated Echo Acquisition Mode (STEAM)[112,113] or 90°−180°−180° excitation Point Resolved Spatial Selection (PRESS)[114] were developed. The STEAM technique can be used with shorter echo times but is disadvantaged by a low signal-to-noise ratio. The pulse sequences most frequently used are single-voxel or chemical shift imaging (CSI) techniques for localized MRS. Proton MRS undertaken with long or short echo times allows the identification of potentially diagnostic and prognostic metabolites.[115−124]

Prior to 1995, implementation of neurospectroscopy was restricted to those laboratories where the radiologist and physicist worked as a team. However, in 1995 there was FDA approval for a fully automated MRS sequence for neurospectroscopy called PROBE (Proton Brain Examination). The methodology allowed neurospectroscopy examinations to be interleaved with MRI sequences. Dr. Brian Ross (Huntington Medical Research Institute, Pasadena, CA) pioneered the application of clinical neurospectroscopy in the United States and around the world. He and his colleagues were responsible for much of the translation of this technology into a routine clinical tool. His goal was to train clinicians to know enough about MRS to request, read, and interpret neurospectroscopy. Ross, along with Heerschap and others,[125−127] documented the changes in the chemistry of the human brain during development and aging.

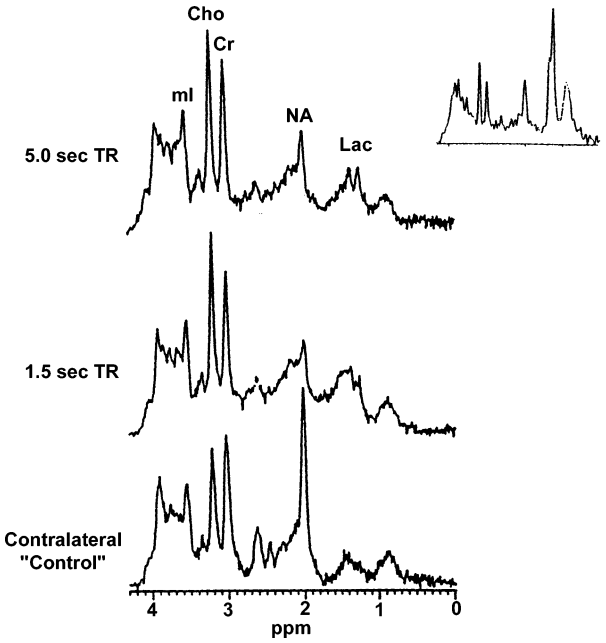

Figure 17. A primary brain tumor showing absent NAA; increased (Cho/Cr), and particularly longer TR, increased lactate (all echo times 30 ms). The inset is from a second patient showing the classical profile of lipid plus lactate, probably recurrence posttherapy. Reprinted with permission from ref 153. Copyright 1999 Marcel Dekker Inc.

The assignment of MR resonances of a primary brain tumor (at 2 different TR values) using the STEAM method at 1.5T is shown in Figure 17. It is compared with the contralateral control. The NAA is reduced in the tumor region, and the choline is more intense than the creatine. Typical spectra using the PRESS method, from brain lesions determined to be astrocytoma, glioma, lymphoma, and metastasis, are compared to those spectra obtained from a region affected by stroke and that of a healthy control in Figure 18. It can be seen that, in a stroke patient, the lactate doublet is inverted and there is a reduction in the intensity of the NAA. In the spectra from glioblastoma and low-grade astrocytoma the choline and creatine resonances are significantly increased compared to that of the NAA. In the spectrum from a metastasis in the brain the NAA signal remains reasonably intense, but choline and creatine resonances have increased, and there is lactate present in the spectrum indicative of the presence of anaerobic metabolism. The lymphoma spectrum is unique in that it has an intense choline resonance and virtually no NAA and the lactate doublet is observed.

Single-voxel ^{1}H MRS is limited to studying data from a single region of interest and does rely upon MRI to provide the spatial location of the information. Recently, the combination of multi-voxel spectroscopy imaging techniques provides 2D information across selective regions.[128−132] For reviews see refs 133 and 134.

The Barcelona group led by Dr. Carles Arós used single-voxel ^{1}H MRS incorporated in a standard imaging study.[135] They studied 37 patients with

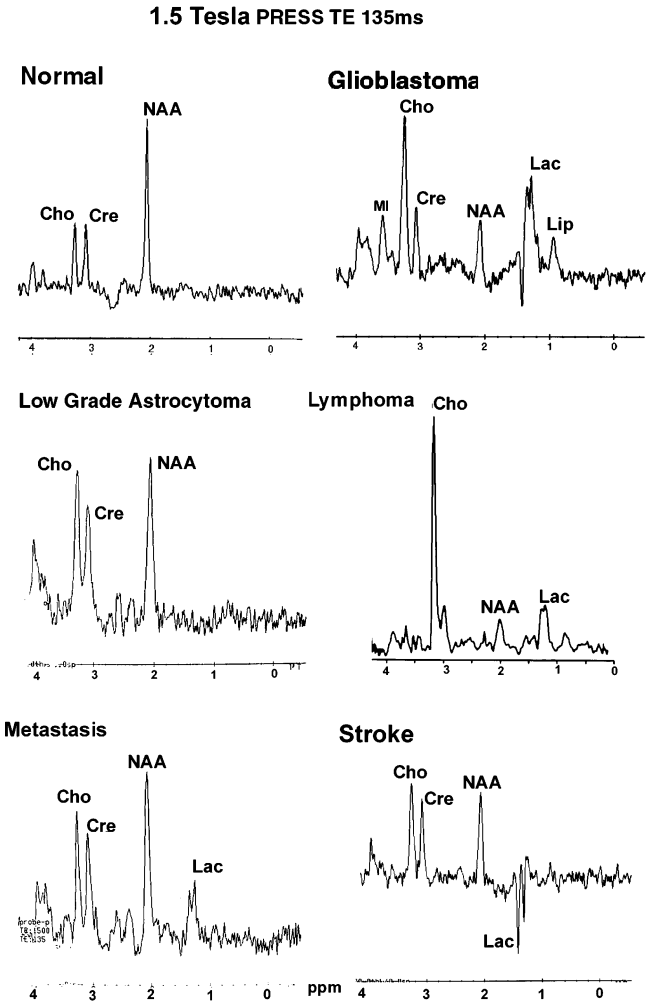

Figure 18. In vivo brain spectroscopy at 1.5T, PRESS, TE = 135 ms: (A) normal brain; (B) glioblastoma; (C) low-grade astrocytoma; (D) lymphoma; (E) metastasis; (F) stroke (Dzendrowskyj, T., Himmelreich, U., Mountford, C., unpublished data).

atypical brain meningiomas and compared them with 93 patients with other intracranial brain neoplasms. The resonances of interest, including those of lactate, alanine, NAA, glutamate, glutamine, creatine, choline, and phosphocreatine, were normalized, statistical differences between the groups analyzed, and algorithms developed. The method had a 94% success in distinguishing between meningioma and other tumors.

The University of California, San Francisco (UCSF) group have undertaken over 1100 MRSI studies and report "the ability to obtain the 3D distribution of the metabolites to be critical for an accurate assessment of metabolic status within the lesion and adjacent tissues".[108]

Neurospectroscopy is now undertaken around the world as is reported in the literature (Spain,[136−138] Turkey,[139] Germany,[140] India,[141] United Kingdom,[142] Poland,[143] and the U.S.[74,144,145]).

Prost and colleagues undertook single-voxel MRS exams (PRESS and CHESS) of the brain from the mid-1990s onward.[146,147] In an interesting study they investigated the accuracy of visual inspection of the MRS data and correlated the findings with histology. The sensitivity and specificity of the exam were 95% and 100%, respectively, for non-blinded analysis. When blinded (using four readers), however, the sensitivity and specificity dropped to 85% and 74%, respectively.[146]

The neurospectroscopy method has to date mainly been interpreted by visual inspection and resonance ratios. Automated techniques for quantitated assessment of MRS[148,149] and of MRSI have also been demonstrated.[145] Arnold and colleagues have used pattern recognition methods to analyze ^{1}H MRSI data. They found the combination allowed discrimination from tissue from the five most common types of supratentorial tumors found in adults. Furthermore, they were able to predict pathological characteristics that were useful in guiding stereotactic biopsy and/or selected tumor reception. They were able to predict with reasonable accuracy which voxels contained necrotic tissue (80%), and the distinction could be made with the presence of tumor cells with and without pleomorphism. There were not sufficient cases examined for any conclusions to be reached about the sensitivity of the technique.[150,151]

SCS classifiers are now developed with both 1.5 and 3T data for healthy brain and specific brain regions such as prefrontal cortex, anterior cingulate cortex, and thalamus (Stanwell, Somorjai, Woodhouse, Mountford, unpublished data) for healthy brain and for patients with pain.[152]

Finally, on the subject of neurospectroscopy there are now reports that the method is able to characterize untreated gliomas using the MRSI methodology.[134] The goal here is to improve planning for focal therapy, guide biopsies, and monitor patients after treatment.[144] While this review is restricted to the application of MRS to cancer, the applications of neurospectroscopy to other diseases and brain function are well described in the text by Ross and Danielson.[153]

4.2. Prostate

The use of serum prostate-specific antigen (PSA) testing and transrectal ultrasound (TRUS) guided biopsy has allowed a significant increase in screening for prostate cancer with increased numbers of patients identified as having disease at an earlier and, therefore as folklore would have it, potentially treatable stage.[154] As described in section 2.2 many men die with prostate cancer but not necessarily from the disease. The decision on how to manage prostate disease once identified can cause a dilemma for both the doctor and patient. Since prostate cancers demonstrate a range of biological potential, the options facing the patient are clinical observation, hormone deprivation therapy or surgical procedures, and radiation or cryosurgical therapies.[148,149] For some patients the cancers will grow so slowly they will never threaten life. For others the disease may progress so rapidly that intervention is required but ineffectual. Thus, the clinical question is which men need to be cured and which men can be cured. The accuracy of the MRS method for identifying the type and extent of prostate biopsies is described in section 2.2. While there is a high level of accuracy achievable using MRS to analyze a biopsy specimen, can this information be obtained *in vivo*?

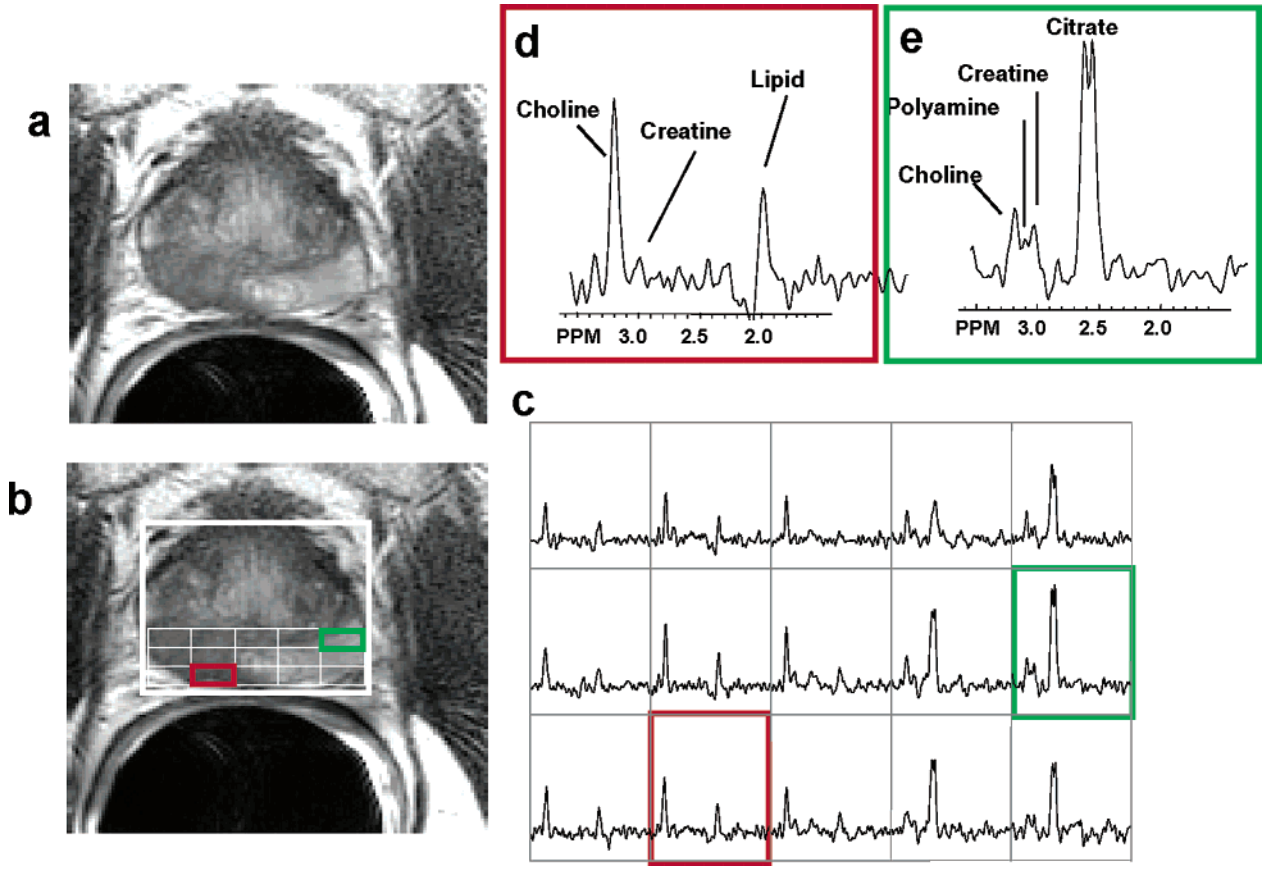

Figure 19. In vivo prostate MRI and MRSI at 1.5T: a representative reception-profile-corrected T_2-weighted FSE axial image taken from a volume data set demonstrating a large tumor in the right midgland to the base. Key: (a) selected volume for the hypointense lesion in the right midgland; (b) overlay of the spectral grid; (c) corresponding spectral array from (b). Regions of cancer (d, red box) demonstrate dramatically elevated choline and a reduction or absence of citrate and polyamines relative to regions of healthy peripheral zone tissue (e, green box). The strength of the combined MRI/MRSI exam is demonstrated when changes in all three metabolic markers (choline, polyamines, and citrate) and imaging findings are concordant for cancer. Reprinted with permission from Kurhanewicz, J., Swanson, M. G., Nelson, S. J., Vigneron, D. B. *J. Magn. Reson. Imaging* **2002**, *16*(4), 451−63. Copyright 2002 Wiley-Liss, Inc., a subsidiary of John Wiley & Sons, Inc.

The UCSF group led by Kurhanewicz, Nelson, and colleagues has spearheaded the *in vivo* prostate program in the U.S. In Europe, Heerschap and colleagues have worked in parallel to put prostate spectroscopy into the clinic *in vivo*. The implementation of prostate MRS will conceivably be the most difficult of all the *in vivo* applications due to the complexity of the zonal anatomy of the prostate and the often multifocal nature of prostate cancer. As with the brain, single-voxel spectroscopy (SVS) was initially developed. An endorectal coil was used which allowed relatively high resolution anatomical images in a reasonable amount of time.[155−162]

Using the UCSF method, lipid was suppressed, both inside the voxel of interest and outside the voxel of interest. High levels of citrate indicated the presence of healthy tissue. Malignant tissue was characterized by low levels of citrate together with increased levels of compounds involved in phosphatidylcholine and phosphatidylethanolamine synthesis and hydrolysis (choline, phosphocholine, glycerolphosphocoline, ethanolamine, and phosphoethanolamine) contributing to the *in vivo* measurement of choline.

Heerschap and colleagues, who focused on spermine (3.0 and 3.3 ppm) as a marker of prostate malignancy, found that at 1.5T it was obscured by choline (3.2 ppm) and creatine (3.0 ppm).[46]

Ackerstaff *et al.*[66] associated these increased choline compounds with increased malignant transformation of human prostatic epithelial cells. However, as described in section 2.2 the interpretation of *in vivo* spectra from the prostate was not simple or straightforward. This resulted in a wide range of accuracies in the literature.[163] The issue was further complicated by the release of software which did not, in many users' hands, provide the accuracies reported by the UCSF group. Thus, once again, and as with the biopsy program, the translation of the MRS technology into the clinic is difficult and requires a high level of acceptance testing (section 6).

Nevertheless, the difficulties of translating this technology into the clinic should not undermine the outstanding contribution made by the UCSF team. The combined use of MRI/MRS for many patients has identified a cancer missed by digital rectal examination and ultrasound (section 5).

A major breakthrough came with the development of MRSI (see ref 108 for a review). The MRSI method produces a three-dimensional (3D) map of contiguous volumes of about 0.24−0.34 cm^3 of voxels that map the entire prostate. Furthermore, as the MRSI and

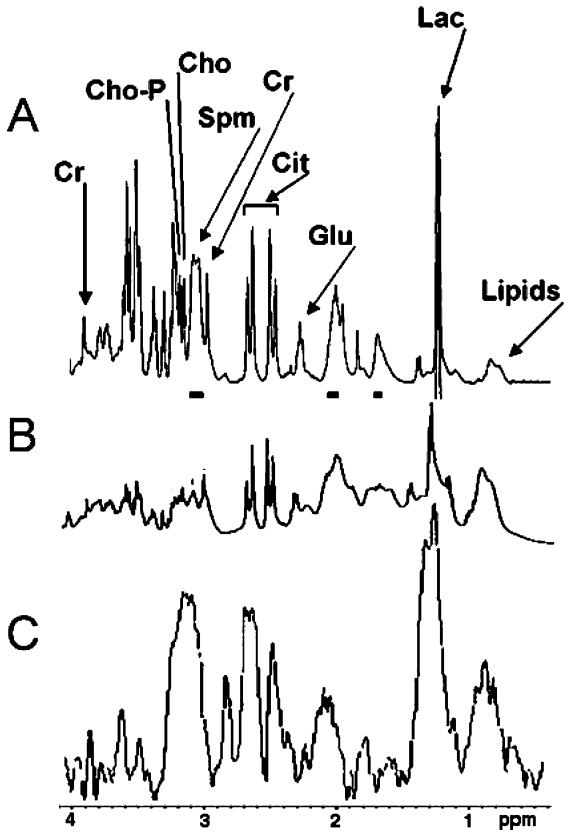

Figure 20. ^{1}H MR spectra of healthy prostate: (A) *ex vivo* MAS at 9.4T; (B) *ex vivo* at 8.5T; (C) *in vivo* 3T whole body scanner. (A) is reprinted with permission from ref 47. Copyright 2001 Elsevier (B) and (C) are from unpublished data of R. Bourne, P. Stanwell, and C. Mountford.

MRI are acquired within the same examination the alignment is easily made. Shown in Figure 19 is an MRSI exam of a patient with cancer. It can be seen in section d that the citrate resonance is totally absent, but there is a strong choline resonance apparent. In section e there is an intense citrate resonance, and while choline and creatine are present, their resonances are significantly smaller than the citrate resonance.

The goal now is to combine the knowledge acquired using high-field 8.5T MRS on tissue specimens with meticulous histological examination[22] and the accurate registration method of MRSI. This combined with analysis of the data with the SCS method should, in principle, allow diagnosis of relatively small lesions. It remains to be seen, however, whether this information can be obtained at 1.5T or whether the higher field 3T magnet is needed to provide the required resolution.

With this in mind, in Figure 20 the spectra from healthy prostate tissue are shown. The comparison is made between the spectrum obtained with the magic angle spinning (MAS) method (9.4T) and the conventional 1D spectrum (8.5T) both obtained on an intact biopsy specimen (parts A and B, respectively, of Figure 20). This is compared with the spectrum obtained from a healthy prostate in a 3T whole body scanner (Figure 20C) (Bourne, R.; Stanwell, P.; Mountford, C., unpublished data) but using only a surface-phased array coil. While the 3T *in vivo* data show broader resonances, the chemical signature of the healthy tissue is apparent. It is expected that with the introduction of endorectal coils for use at 3T the resolution and signal-to-noise ratio will be sufficient for highly accurate pathological diagnosis of prostate disease. However, visual inspection of the data will not be sufficiently accurate to allow the various pathologies to be discerned. With the implementation of the SCS method, the pathology and the volume of each tumor and tissue type should be achievable.

4.3. Breast

If the spatial location(s) and pathology of breast lesions could be determined prior to surgery, it would allow preoperative decisions regarding patient management. Improvements in dynamic contrast enhancement features of breast tumors and the appreciation of morphological characteristics of these lesions have improved the accuracy of the MRI method.[164−173] However, the application of *in vivo* MRS to breast has some way to go. In this review is included an explanation of why the authors consider the present methodology to be inadequate for clinical use at 1.5T.

The first report of *in vivo* ^{1}H MRS at 1.5T of breast tumors was by Sijens and colleagues.[174] They used PRESS, and their work suggested that cancers had higher water-to-fat ratios than normal tissue.[174] This observation was later refuted in a study by Roebuck[175] using a STEAM sequence (Figure 21). The study by Roebuck did show the presence of a broad composite resonance at 3.2 ppm, containing choline in 7 of 10 malignant tumors and also in 1 of 7 benign lesions. One particular false positive was a large tubular adenoma, a relatively rare tumor, but at large size considered to be a borderline malignant lesion.[176]

In other studies undertaken at 1.5T Yeung[177] showed the presence of the composite resonance at 3.2 ppm in choline in 22 of 24 malignant lesions and 1 of 6 benign lesions (sensitivity and specificity of 91.7% and 83.3%, respectively). Kvistad, Gribbestad and colleagues[178] (Figure 22) reported the same composite resonance at 3.2 ppm in 9 of 11 malignant breast cancer lesions and 2 of 11 benign lesions (sensitivity and specificity of 81.8% and 75.9%, respectively). Of note was the report that this composite resonance containing choline was observed in 5 of 7 lactating women but in none of 11 apparently normal volunteers (Table 1). Similar accuracies were reported by Cecil[179] (sensitivity and specificity of 82.6% and 86.7%, respectively), and Jagannathan and colleagues (sensitivity and specificity of 78.2% and 85.7%, respectively).[180] Of these studies, Kvistad and colleagues[178] were the only group where 11 normal volunteers were examined. None were false positives.

A study which investigated 40 apparently healthy volunteers, 3 lactating women, and 14 women with carcinoma of the breast questioned the reliability of using the composite choline resonance at 3.2 ppm (as a marker for cancer).[181] Two of the lactating volunteers and 3 of the 40 apparently healthy volunteers recorded the 3.2 ppm composite resonance. Eleven

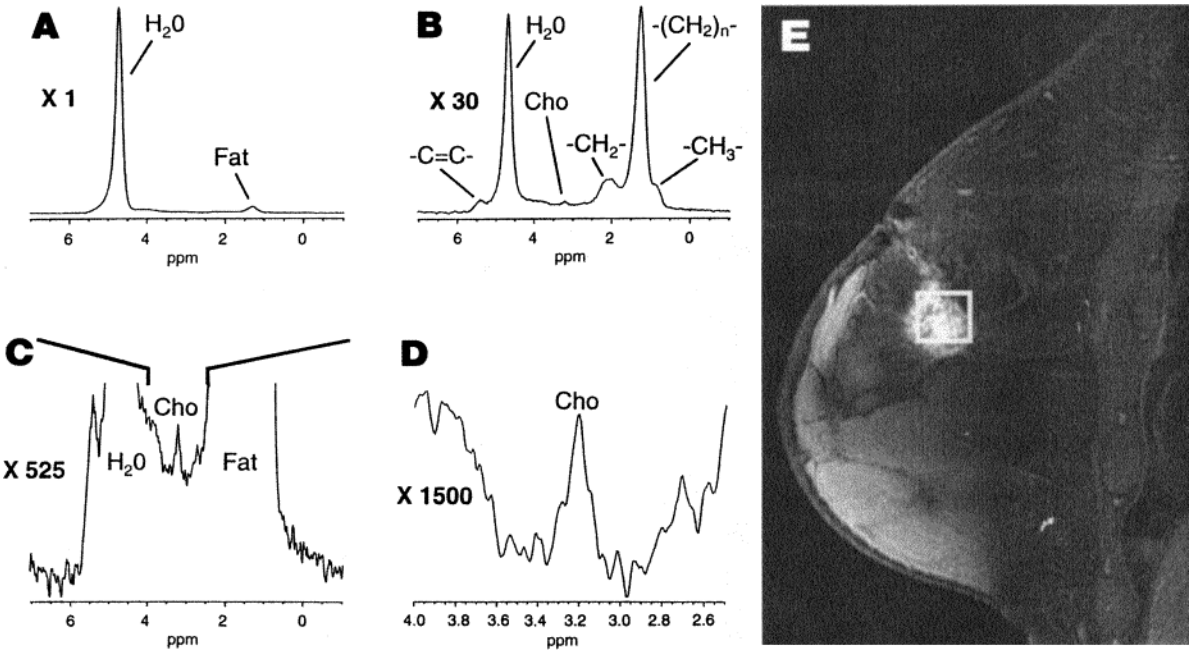

Figure 21. In vivo breast MRS at 1.5T. (A) Unsuppressed and (B−D) suppressed MR spectra (TR = 2000, TE = 31) of intraductal and infiltrating ductal carcinoma show resonance assignments for H_2O, fat, and Cho. (E) The gadolinium-enhanced MR image (TR = 28, TE = 4) shows the tumor and the voxel used for MR spectroscopy. In (A)−(D), scale factors are relative to the unsuppressed spectrum. The nominal voxel volume was 1.6 cm^3. In (A)−(D), "X" indicates the magnification. Reprinted with permission from ref 175. Copyright 1998 Radiological Society of North America.

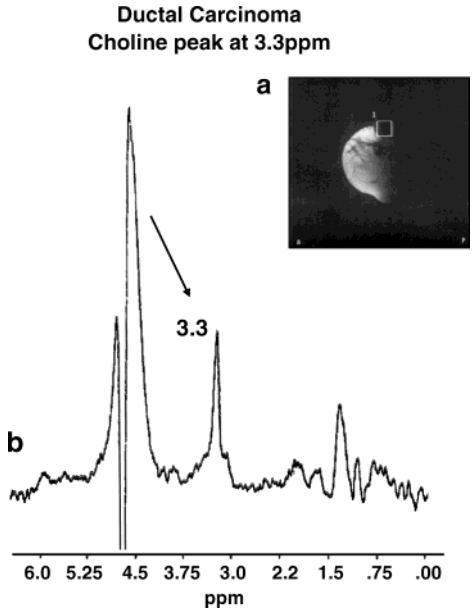

Figure 22. (A) Sagittal MRI (1.5T) of a 65 year old patient with a ductal carcinoma and (B) [1]H MR spectrum of a 20 × 20 × 20 mm^3 voxel (256 averages), showing the intense signal at 3.3 ppm. Reprinted from Gribbestad, I. S.; Singstad, T. E.; Nilsen, G.; Fjosne, H. E.; Engan, T.; Haugen, O. A.; Rinck, P. A. *J. Magn. Reson. Imaging* **1998**, *8*, 1191−1197. Copyright 1998 Wiley-Liss, Inc., a subsidiary of John Wiley & Sons, Inc.

of the 14 cancer patients also recorded the presence of the resonance at 3.2 ppm. This resulted in a sensitivity of 79% and a specificity of 88%.

It was demonstrated by Aboagye and colleagues that total choline-containing phospholipid metabolite levels increase with progression from normal to immortalized to oncogene-transformed to tumor-derived cells.[52] It has also been shown from MR spectra that fibroblasts[182] contain low levels of choline and creatine. Immortalized and aging cells[31] contain increasing levels of choline and to a much lesser extent creatine. Thus, for the MRS method to provide the accuracies recorded at the higher field strength of 8.5T on biopsy material, more resonances than the composite at 3.2 ppm[183] need to be resolved for accurate diagnosis.[14] This may be more readily achievable at the higher field strength of 3T.

4.4. Thyroid

A purpose-designed multi-ring surface coil was built for undertaking *in vivo* MRS of the thyroid.[184] A coil was wound for both 1.5 and 3T scanners. The typical spectrum collected using this coil at 3T from a solitary thyroid nodule is shown in Figure 23. Figure 23A is a T_1-weighted axial image of a thyroid lesion with the corresponding *in vivo* [1]H MR spectrum shown in Figure 23B. For comparison, Figure 23C shows the *ex vivo* [1]H MR spectrum of a thyroid biopsy specimen of the same pathology recorded at 8.5T. The spectroscopic data shown in Figure 23B confirm the lesion to be a benign adenoma on the basis of the *ex vivo* MRS studies. This diagnosis was confirmed histologically. This technology was attempted at the lower frequency of 1.5T, but the spectral resolution was less than optimal. The clinical future of MRS of the thyroid at 3T looks promising.

4.5. 2D Spectroscopy

The benefits of using 2D spectroscopy were described in sections 3.1 and 3.2. Thomas and colleagues have implemented a series of 2D spectroscopy sequences for *in vivo* use,[185] allowing diagnostic and prognostic markers to be identified. In the case of the brain[186] those resonances that were composite in the 1D spectrum were resolved into discrete cross-peaks

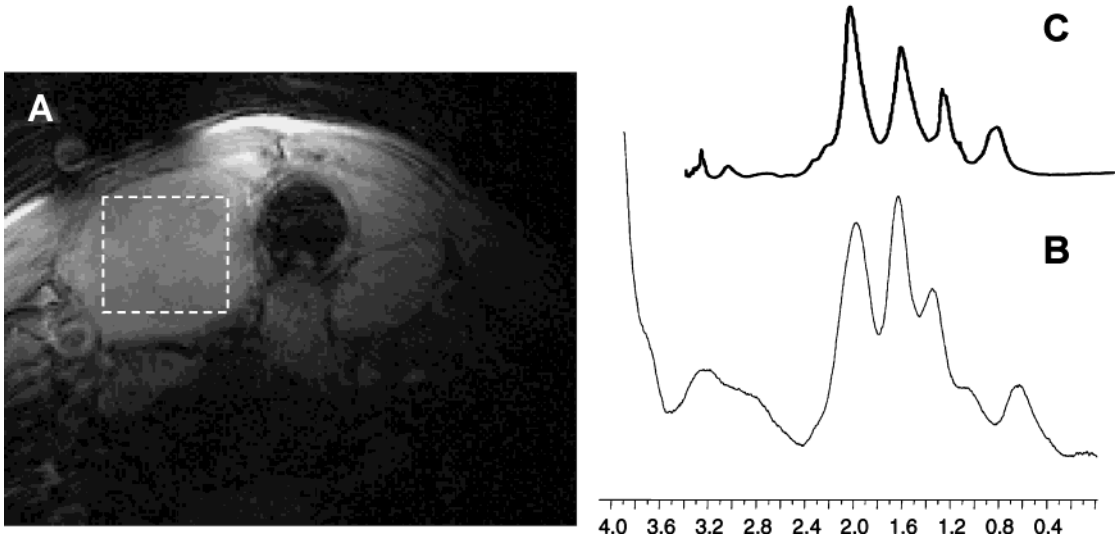

Figure 23. ^{1}H MR on benign follicular adenomas of the thyroid: (A) *in vivo* T_1-weighted axial image; (B) corresponding *in vivo* ^{1}H 3T MR spectrum (undertaken at the National Research Council of Canada, Winnipeg; data were obtained using a specially designed multiring surface coil); (C) *ex vivo* ^{1}H 8.5T MR spectra from a biopsy specimen of the same pathology. Reprinted with permission from Mountford, C. E.; Doran, S. T.; Lean, C. L.; Russell, P. *Biophys. Chem.* **1997**, *68*, 127−135. Copyright 1997 Elsevier.

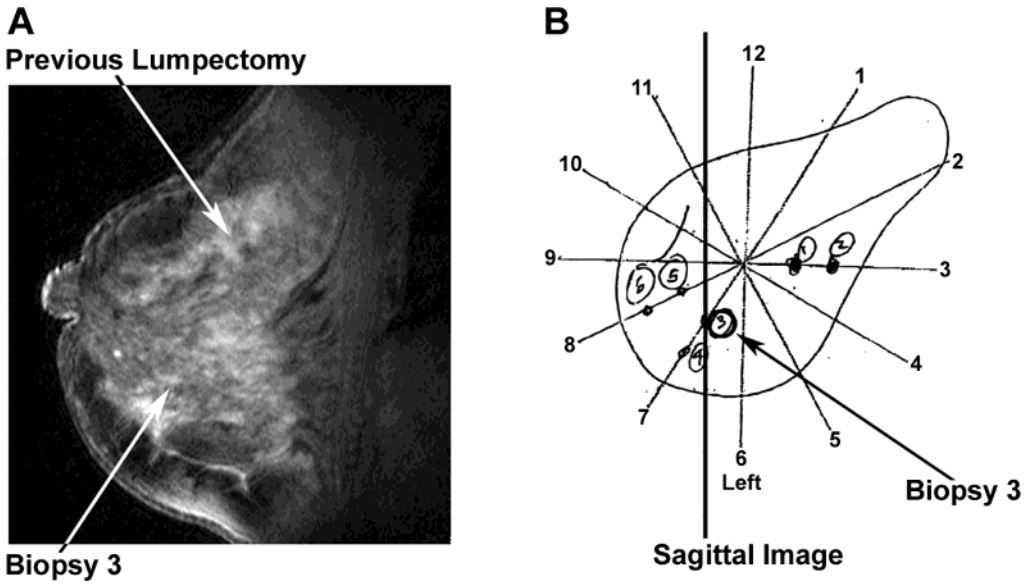

Figure 24. (A) Sagittal gadolinium-enhanced 1.5T MR image of the breast. The site of the previous lumpectomy and site of fine-needle biopsy no. 3 are indicated by the arrows. The diffuse white areas represent residual DCIS post lumpectomy. (B) A schematic showing the position of the sagittal image shown in (A) and the sites of fine-needle biopsies. (Stanwell, P., Boyages, J., Sinclair, E., Baker, L., Mountford, C., unpublished data.)

in the second dimension. In the case of human breast cancer 2D spectroscopy facilitated the separation of diagnostic and prognostic markers such as choline from the variable fat content[187] (see sections 2.3 and 4.4).

In keeping with the knowledge that as spectroscopy becomes a reliable tool for the diagnosis of diseases its reproducibility is of paramount importance, Thomas and colleagues investigated the reproducibility of 2D COSY in healthy human brain.[188] Thomas and colleagues have now started to implement 2D spectroscopy *in vivo* for the elucidation of disease mechanisms. For example, they have used 2D *J*-resolved spectroscopy to distinguish between cancer and benign tissue at 1.5T. Spermine was clearly separated from choline and creatine using this method.[189]

5. Case Studies Combining in Vivo MRI/MRS and MRS on Biopsy

5.1. Breast

A 50 year old female was referred having had two previous lumpectomies, both with positive margins (i.e., the surgeon did not manage to remove all of the diseased tissue). The pathology of the two previous lumpectomies was DCIS without microinvasion. The extent of disease and the diagnosis were queried.

Examinations undertaken included gadolinium-enhanced MRI (1.5T), which showed diffuse disease (see Figure 24). On the left-hand side is a T_2-weighted image, and on the right-hand side is the schematic diagram prepared by the pathologist following mastectomy.

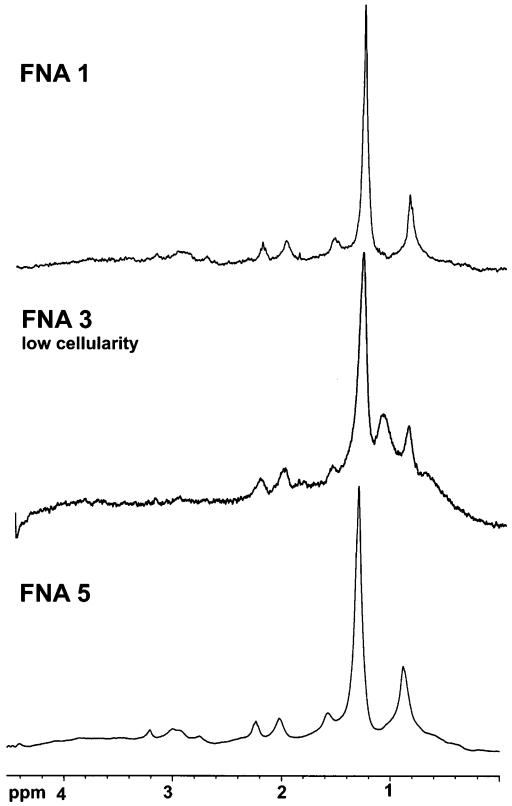

Figure 25. Ex vivo [1]H MR spectra (8.5T, 37 °C) of fine-needle biopsy specimens from the breast (MRI image shown in Figure 24). Spectra from regions 1, 3, and 5 as indicated in the schematic in Figure 24 are shown.

Ultrasound-guided FNABs were obtained from six regions as shown in Figure 24. The biopsies were examined at the higher field strength of 8.5T. Three of the six biopsies were determined by *ex vivo* MRS analysis to be benign. These were the biopsies taken from the spatial locations marked 2, 4, and 6. The spectra obtained from the biopsies taken from regions 1, 3, and 5 are shown in Figure 25. Comparing these spectra with those in Figure 5, i.e., DCIS with and without microinvasion, all 3 biopsies were typical of DCIS without microinvasion. Thus, a diagnosis of extensive diffuse disease was identified by gadolinium-enhanced MRI. The pathology was determined to be DCIS without microinvasion using *ex vivo* MRS. Following this report the surgeon recommended mastectomy and breast reconstruction. Following mastectomy the pathology was confirmed as DCIS without microinvasion (Stanwell, P.; Boyages, J.; Sinclair, E.; Baker, L.; Mountford, C., unpublished data).

5.2. Prostate

A 69 year old man was referred for MRI and MRS of the prostate. He had PSA levels rising from 6.0 to 7.7 over an 11 month period. Bladder function was normal and the prostate was palpably normal. The ultrasound examination proved negative.

The examinations undertaken included MRI and MRS at 1.5T, ultrasound-guided biopsies to the region identified by the MR exam, and high-field (8.5T) MRS of the biopsy material. The T_2-weighted axial image in Figure 26 demonstrates a hypo-intense lesion in the left peripheral zone; *in vivo* MRS showed elevated levels of choline in the same region. The targeted biopsy was examined by both conventional histopathology and high-field MRS. Both confirmed the presence of cancer. In this case the diagnosis of adenocarcinoma with perineural invasion was given. If it were not for the MR examination, this patient's cancer would have been missed.[190]

5.3. Brain

A 70 year old man was referred having previously been diagnosed with a cerebral glioma. He had been treated by radiotherapy, but another lesion in a different location was detected two weeks after radiotherapy had ceased. The query was whether this

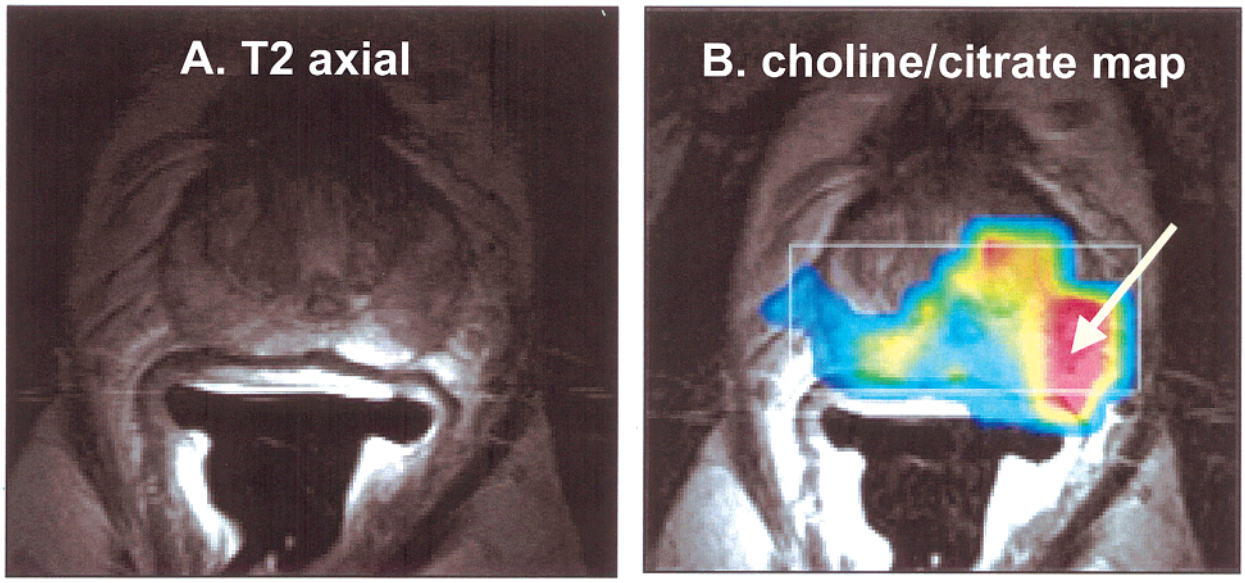

Figure 26. In vivo 1.5T [1]H MR images of the prostate. (A) The T2W axial image demonstrates a hypointense lesion in the left peripheral zone. (B) The overlaid metabolite map confirms the presence of an altered choline/creatine ratio in the same peripheral zone region. The targeted biopsy in the region shown in red reveals prostate cancer with perineural invasion.

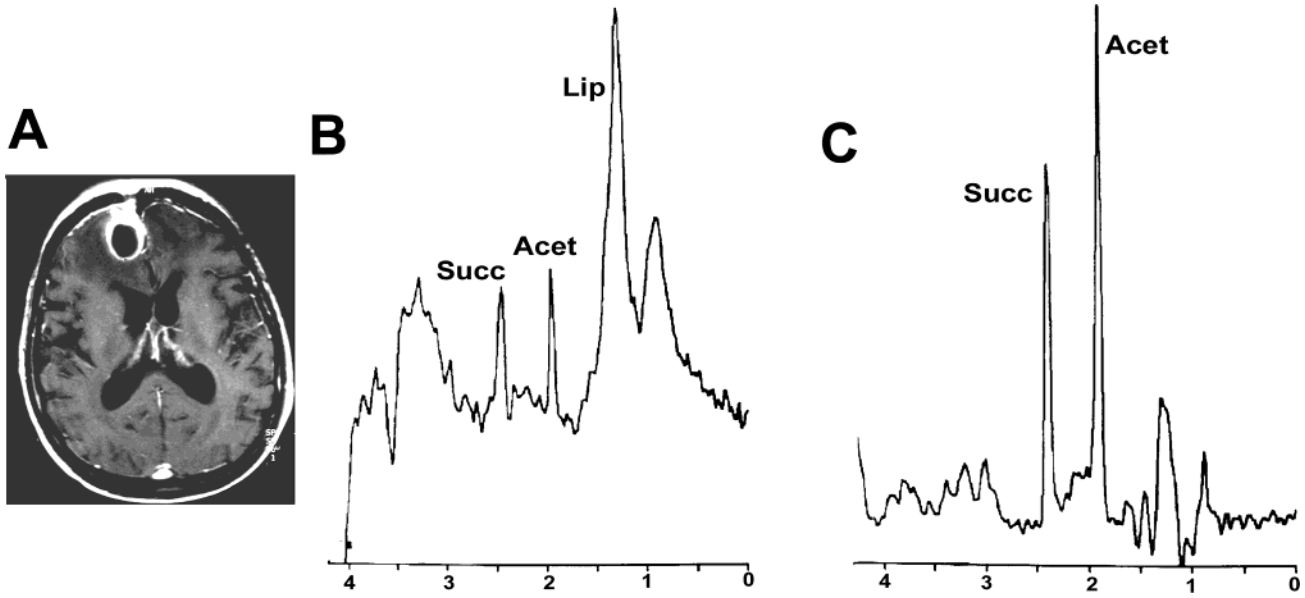

Figure 27. In vivo 1.5T ^{1}H MR of a human brain lesion. (A) The MR image shows partial ring enhancement of the lesion following gadolinium injection. (B) STEAM (TE = 20 ms) demonstrates the absence of an NAA signal with the presence of signals from lipids, succinate, and acetate. C) PRESS (TE = 135 ms) demonstrates the presence of acetate and succinate. (Himmelreich, U., Sorrell, T., Mountford, C., unpublished data.)

second lesion was radiation necrosis or recurrent tumor. The spatial location of the new lesion was located by gadolinium-enhanced T_1-weighted imaging where a ring-enhancing lesion was identified, as seen in Figure 27. Single-voxel spectroscopy was undertaken using the STEAM experiment with a TE of 20 ms at 1.5T and PRESS at 135 ms. The presence of succinate and acetate identified a mixed bacterial abscess, *Streptococcus milleri* and anaerobe gram-negative bacteria. The patient, who was successfully treated with antibiotics, did not need to have a biopsy due to the positive diagnosis of an abscess by the *in vivo* MRS method (Himmelreich, U.; Sorrell, T.; Mountford, C., unpublished data).

6. Translation into the Clinic and Clinical Acceptance Testing

For MRS to be implemented effectively and with a high level of accuracy, the technology needs to be transferred from the academic medical centers into routine hospital use. This could be the most difficult part of the entire operation. As described at the beginning of this review house-keeping issues, such as the wrong plastic used for collection vials and syringes and a lack of understanding by other laboratories of the importance of storing specimens, caused failure by some sites to repeat the biopsy data collection. While the use of neurospectroscopy was implemented with apparently relative ease, this only occurred due to the significant time and effort of Dr. Ross and colleagues, who were devoted to teaching programs worldwide.

Difficulty was also experienced by the UCSF team when they attempted to role out their prostate spectroscopy program to other centers with the assistance of a commercial partner.

For the biopsy program, collection kits need to be made available, hardware needs to be automated, and robust software needs to be incorporated such that data collection and comparison with the mathematical classifiers are part of an automated system. Methods of reporting, diagnosis, and prognosis must fit neatly into standard pathological reporting processes. For the *in vivo* programs, coils, experimental protocols, and automated data collection programs need to be robust.

Acceptance testing of either biopsy or *in vivo* spectroscopy needs to be undertaken with rigor. Three or four well-qualified test sites need to be identified where radiologists, pathologists, and surgeons are all world leaders in a particular discipline. The technology needs to be integrated by the medical profession into routine patient management and a review of the worth of the test with the current diagnostic methods provided. Critical feedback should be sought during the testing period of whether the technology addresses a perceived need in the diagnostic process, provides advantages over current diagnostic techniques (accuracy, robustness, cost), and, finally, provides data useful for patient management. Prior to the commencement of each of these acceptance testing programs, the site where the technology was predominantly developed needs to be integrally involved until all problems are resolved. Only then can reliable acceptance testing commence.

It has been our experience that when technology such as MRS has a genuine contribution to make to diagnosis of disease and patient management medical specialists embrace the technology. However, for MRS to be effectively introduced into the clinic, the most elementary of house-keeping duties need to be acknowledged. Quite often scientists are the wrong people to implement translation of their own technology into the clinic. The radiologists and the pathologists who are attuned to routine patient management are best equipped for this responsibility. A commercial partner who is understanding of the need for

such a robust introduction of a new technology is a necessity.

7. Conclusions

In the last 25 years spectroscopy has gone from being the physicist's playground to being an integral part of a modern clinical assessment procedure.

Neurospectroscopy is regularly used in the clinic interleaved with routine MRI sequences. Currently, *in vivo* spectroscopy of the prostate and breast are only available to patients with access to a few university radiology departments around the world. It is anticipated that by adding the robust mathematical classifiers to the now well-tested pulse sequences the *in vivo* MRS technology could be released for use on commercial systems in the not too distant future.

Proton MRS is now poised to be introduced into the pathology laboratory as an adjunct to, and in some cases replacement for, the difficult pathologies such as follicular adenoma of the thyroid and Barrett's esophagus. The combination of MRI and MRS *in vivo* with correlative MRS on biopsy currently offers an unprecedented accuracy for the diagnosis and prognosis for human diseases.

8. Abbreviations

^{13}C	carbon-13
1D	one-dimensional
^{1}H	proton
2D	two-dimensional
3D	three-dimensional
AA	Hα of amino acid residues
acyl	acetyl residues
Ala	alanine
BPH	benign prostatic hyperplasia
CHESS	chemical shift selective saturation
CHOH	carbohydrate residues (mainly glucose residues from glycogen and free glucose)
Chol	choline
Chols	choline-containing metabolites
CIN	cervical intraepithelial neoplasia
Cit	citrate
COSY	COrrelated SpectroscopY
Cre	creatine
CSI	chemical shift imaging
DCIS	ductal carcinoma *in situ*
FNABs	fine-needle aspiration biopsies
GABA	γ-aminobutyric acid
Glc	α- and β-glucose residues
Glu/Gln	glutamate/glutamine
GPC	glycerolphosphocholine
HCC	hepatocellular carcinoma
H and E	haematoxylin and eosin
His	histidine
HSQC	heteronuclear single-quantum coherence
IBD	Institute for Biodiagnostics
Ile	isoleucine
Inos	inositol
Lac	lactate
LDA	linear discriminant analysis
Leu	leucine
LGA	linear regression analysis
Lip	lipid
Lys	lysine
MAS	magic angle spinning
MRI	magnetic resonance imaging
MRS	magnetic resonance spectroscopy
MRSI	magnetic resonance spectroscopic imaging
NRC	National Research Council, Canada
OVS	outer volume suppression
PC	phosphocholine
PIN	prostate intraepithelial neoplasia
PRESS	excitation point resolved spatial selection
PROBE	proton brain examination
PSA	prostate-specific antigen
SCS	statistical classification strategy
SVS	single voxel spectroscopy
SNR	signal-to-noise ratio
STEAM	stimulated echo acquisition mode
Tau	taurine
Thr	threonine
TRUS	transrectal ultrasound
UCSF	University of California—San Francisco
UDP-hexose	uridine diphosphate hexose
Val	valine

9. Acknowledgments

We acknowledge the long-term contributions from the other clinical and scientific directors of the IMRR, Prof. Martin Tattersall, Drs. Uwe Himmelreich and Peter Malycha, and Prof. Tania Sorrell. We gratefully acknowledge the contributions made by our colleagues at the NRC, Winnipeg, Drs. I. C. P. Smith, Ray Somorjai, Brion Dolenko, Slavek Tomanek, Scott King, and S. Nikulin. We thank Drs. Brian Ross, Stefan Bluml, Bob Lenkinski, Mary Hockman, Ingrid Gribbestadt, and John Kurhanewicz for sharing their thoughts and goals with us. We thank Drs. Roger Bourne and Philip Katelaris for their contribution to the prostate program, Dr. David Clark for his contribution to the breast program, Ms. Susan Dowd for her tireless specimen management, and present and past staff and students within the Department of Magnetic Resonance of Medicine. We thank Ms. Brooke O'Donnell and Dr. Deborah Edward for helping prepare this manuscript. We thank our colleagues and friends from around the world for allowing us to describe their work and for their many interesting discussions and contributions to this review. Last, but not least, we thank Prof. T. S. Reeve, Australia's preeminent surgeon, whose guidance and support has been invaluable.

10. References

(1) Block, R. E. *FEBS Lett.* **1973**, *34*, 109.
(2) Ugurbil, K.; Shulman, R. G.; Brown, T. R. In *Biological Applications of Magnetic Resonance*; Shulman, R. G., Ed.; Academic Press: New York, 1979.
(3) Radda, G. K.; Seeley, P. J. *Annu. Rev. Physiol.* **1979**, *41*, 749.
(4) Daniels, A.; Williams, R.; Wright, P. *Neuroscience* **1978**, *3*, 573.
(5) Metcalf, D. *Recent Results Cancer Res.* **1966**, 5.
(6) Mountford, C. E.; Grossman, G.; Gatenby, P. A.; Fox, R. M. *Br. J. Cancer* **1980**, *41*, 1000.
(7) Mountford, C. E.; Grossman, G.; Reid, G.; Fox, R. M. *Cancer Res.* **1982**, *42*, 2270.
(8) Ramshaw, I. A.; Carlsen, S. T.; Hoon, D.; Warrington, C. *Int. J. Cancer* **1982**, *30*, 601.
(9) Mountford, C. E.; Wright, L. C.; Holmes, K. T.; Mackinnon, W. B.; Gregory, P.; Fox, R. M. *Science* **1984**, *226*, 1415.
(10) Mountford, C.; Russell, P. US Patent 5,318,031, 1994.
(11) Mountford, C.; Russell, P.; Smith, I.; Somorjai, R. US Patent PCT Appl. No. PCT/CA00/01238, 2000.
(12) Ernst, R. R.; Anderson, W. A. *Rev. Sci. Instrum.* **1966**, *37*, 93.
(13) Cross, K. J.; Holmes, K. T.; Mountford, C. E.; Wright, P. E. *Biochemistry* **1984**, *23*, 5895.

(14) Lean, C. L.; Somorjai, R. L.; Smith, I. C. P.; Russell, P.; Mountford, C. E. In *Annual Reports on NMR Spectroscopy*; Webb, G., Ed.; Academic Press: New York, 2002; Vol. 48.
(15) Mountford, C. E.; Lean, C. L.; Mackinnon, W. B.; Russell, P. In *Annual Reports on NMR Spectroscopy*; Webb, G. A., Ed.; Academic Press: New York, 1993; Vol. 27.
(16) Mackinnon, W. B.; Russell, P.; May, G. L.; Mountford, C. E. *Int. J. Gynaecol. Cancer* **1995**, *5*, 211.
(17) Delikatny, E. J.; Russell, P.; Hunter, J. C.; Hancock, R.; Atkinson, K. H.; van Haaften-Day, C.; Mountford, C. E. *Radiology* **1993**, *188*, 791.
(18) Lean, C. L.; Newland, R. C.; Ende, D. A.; Bokey, E. L.; Smith, I. C.; Mountford, C. E. *Magn. Reson. Med.* **1993**, *30*, 525.
(19) Russell, P.; Lean, C. L.; Delbridge, L.; May, G. L.; Dowd, S.; Mountford, C. E. *Am. J. Med.* **1994**, *96*, 383.
(20) Barry, P. A.; Wadstrom, C.; Falk, G. D.; Shehan, P.; Russell, P.; Lean, C. L.; Mountford, C. E. In *The Oesophagrogastric Junction*; Giuli, R., Ed.; John Libbey Eurotext: Montrouge, 1998.
(21) Mackinnon, W. B.; Barry, P. A.; Malycha, P. L.; Gillett, D. J.; Russell, P.; Lean, C. L.; Doran, S. T.; Barraclough, B. H.; Bilous, M.; Mountford, C. E. *Radiology* **1997**, *204*, 661.
(22) Swindle, P.; McCredie, S.; Russell, P.; Himmelreich, U.; Khadra, M.; Lean, C., L.; Mountford, C. E. *Radiology* **2003**, *228*, 144.
(23) Mountford, C. E.; Somorjai, R. L.; Malycha, P.; Gluch, L.; Lean, C.; Russell, P.; Barraclough, B.; Gillett, D.; Himmelreich, U.; Dolenko, B.; Nikulin, A. E.; Smith, I. C. *Br. J. Surg.* **2001**, *88*, 1234.
(24) Soper, R.; Himmelreich, U.; Painter, D.; Somorjai, R.; Lean, C.; Dolenko, B.; Mountford, C.; Russell, P. *Pathology* **2002**, *34*, 417.
(25) Gluch, L. Ph.D. Thesis, University of Sydney, Sydney, NSW, Australia, 2002.
(26) Wright, L. C.; May, G. L.; Gregory, P.; Dyne, M.; Holmes, K. T.; Williams, P. G.; Mountford, C. E. *J. Cell Biochem.* **1988**, *37*, 49.
(27) Holmes, K.; Williams, P.; Bloom, M.; Dyne, M.; Mountford, C.; King, N.; Karaman, M.; Ninham, B.; Blanden, R. *Magn. Reson. Med. Biol.* **1988**, *1*, 75.
(28) Lean, C. L.; Mackinnon, W. B.; Delikatny, E. J.; Whitehead, R. H.; Mountford, C. E. *Biochemistry* **1992**, *31*, 11095.
(29) Mackinnon, W. B.; Huschtscha, L.; Dent, K.; Hancock, R.; Paraskeva, C.; Mountford, C. E. *Int. J. Cancer* **1994**, *59*, 248.
(30) Mackinnon, W. B.; Delbridge, L.; Russell, P.; Lean, C. L.; May, G. L.; Doran, S.; Dowd, S.; Mountford, C. E. *World J. Surg.* **1996**, *20*, 841.
(31) Rutter, A.; Mackinnon, W. B.; Huschtscha, L. I.; Mountford, C. E. *Exp. Gerontol.* **1996**, *31*, 669.
(32) Mountford, C. E.; Delikatny, E. J.; Dyne, M.; Holmes, K. T.; Mackinnon, W. B.; Ford, R.; Hunter, J. C.; Truskett, I. D.; Russell, P. *Magn. Reson. Med.* **1990**, *13*, 324.
(33) Mountford, C. E.; Saunders, J. K.; May, G. L.; Holmes, K. T.; Williams, P. G.; Fox, R. M.; Tattersall, M. H.; Barr, J. R.; Russell, P.; Smith, I. C. *Lancet* **1986**, *1*, 651.
(34) Delbridge, L.; Lean, C.; Russell, P.; May, G. L.; Roman, S.; Dowd, S.; Reeve, T. S.; Mountford, C. E. *World J. Surg.* **1994**, *18*, 512.
(35) Delbridge, L.; Lean, C. L.; Russell, P.; May, G. L.; Roman, S.; Dowd, S.; Reeve, T. S.; Mountford, C. E. *World J. Surg.* **1994**, *18*, 512, discussion 516−517.
(36) Lean, C. L.; Delbridge, L.; Russell, P.; May, G. L.; Mackinnon, W. B.; Roman, S.; Fahey, T. J., III; Dowd, S.; Mountford, C. E. *J Clin. Endocrinol. Metab.* **1995**, *80*, 1306.
(37) Mountford, C. E. *Today's Life Sci.* **1998**, 22.
(38) Somorjai, R.; Bourne, R.; Nikulin, A.; Dolenko, B.; Russell, P.; Mountford, C. *Proceedings, Eleventh Scientific Meeting, International Society for Magnetic Resonance in Medicine, ISMRM*, Toronto, Ontario, Canada, 2003; p 762.
(39) van der Hoek, R. *Malignant neoplasms of the prostate*; Disease Registers Unit, Australian Institute of Health and Welfare, Canberra, Australia, 1995.
(40) Hirst, G. H.; Ward, J. E.; Del Mar, C. B. *Med. J. Aust.* **1996**, *164*, 285.
(41) Greenlee, R. T.; Murray, T.; Bolden, S.; Wingo, P. A. *Ca−Cancer J. Clin.* **2000**, *50*, 7.
(42) McNeal, J. E. In *Normal and abnormal growth of the prostate*; Goland, M., Ed.; Thomas: Springfield, IL, 1975; p 750.
(43) McNeal, J. E. *Urology* **1981**, *17*, 11.
(44) McNeal, J. E. *Am. J. Surg. Pathol.* **1988**, *12*, 619.
(45) Hahn, P.; Smith, I. C. P.; Leboldus, L.; Littman, C.; Somorjai, R. L.; Bezabeh, T. *Cancer Res.* **1997**, *57*, 3398.
(46) van der Graaf, M.; Schipper, R. G.; Oosterhof, G. O.; Schalken, J. A.; Verhofstad, A. A.; Heerschap, A. *Magma* **2000**, *10*, 153.
(47) Cheng, L. L.; Wu, C.; Smith, M. R.; Gonzalez, R. G. *FEBS Lett.* **2001**, *494*, 112.
(48) Cole, P.; Rodu, B. In *Cancer. Principles and practice of oncology*; De Vita, V. T., Hellman, S., Rosenberg, S. A., Eds.; Lippincot Williams and Wilkins: Philadelphia, 2001.
(49) Coates, M.; McCredie, M.; Armstrong, B. *Cancer in New South Wales: Incidence and Mortality*; Cancer Control Information Center, New South Wales Cancer Council: Sydney, 1996.
(50) Tabar, L.; Fagerberg, P.; Duffy, S.; Day, N.; Gad, A.; Grontoff, O. *Radiol. Clin. North Am.* **1992**, *30*, 187.
(51) Katz-Brull, R.; Seger, D.; Rivenson-Segal, D.; Rushkin, E.; Degani, H. *Cancer Res.* **1970**, *62*, 2002.
(52) Aboagye, E. O.; Bhujwalla, Z. M. *Cancer Res.* **1999**, *59*, 80.
(53) Lean, C. L.; Russell, P.; Mountford, C. E. *J. Women's Imaging* **2000**, *2*, 19.
(54) Sitter, B.; Sonnewald, U.; Spraul, M.; Fjosne, H. E.; Gribbestad, I. S. *NMR Biomed.* **2002**, *15*, 327.
(55) Cheng, L. L.; Chang, I.-W.; Smith, B. L.; Gonzalez, R. G. *J. Magn. Reson.* **1998**, *135*, 194.
(56) Simonetti, R. G.; Camma, C.; Fiorello, F.; Politi, F.; D'Amico, G.; Pagliaro, L. *Dig. Dis. Sci.* **1991**, *36*, 962.
(57) Duvoux, C. *Ann. Chir.* **1998**, *52*, 511.
(58) Li Volsi, V. In *Surgical Pathology of the Thyroid*; W. Saunders: Philadelphia, 1990; Vol. 9.
(59) Mazzaferri, E. *N. Engl. J. Med.* **1993**, *328*, 553.
(60) Mazzeferri, E. *Am. J. Med.* **1992**, *93*, 359.
(61) Somorjai, R. L.; Nikulin, A. E.; Pizzi, N.; Jackson, D.; Scarth, G.; Dolenko, B.; Gordon, H.; Russell, E.; Lean, C. L.; Delbridge, L.; Mountford, C. E.; Smith, L. C. P. *Magn. Reson. Med.* **1995**, *33*, 257.
(62) Blot, W. J.; Devesa, S. S.; Kneller, R. W.; Fraumeni, J. F. *JAMA, J. Am. Med. Assoc.* **1991**, *265*, 1287.
(63) Clark, G. W.; Smyrk, T. C.; Burdiles, P.; Hoeft, S. F.; Peters, J. H.; Kiyabu, M.; Hinder, R. A.; Bremner, C. G.; DeMeester, T. R. *Arch. Surg.* **1994**, *129*, 609.
(64) Spechler, S. *Semin. Gastrointest. Dis.* **1996**, *7*, 51.
(65) Spechler, S.; Goyal, R. *Gastroenterology* **1994**, *106*, 275.
(66) Ackerstaff, E.; Pflug, B. R.; Nelson, J. B.; Bhujwalla, Z. M. *Cancer Res.* **2001**, *61*, 3599.
(67) Streitz, A. P.; Andrews, C. W.; Ellis, F. H. *J. Thorac. Cardiovasc. Surg.* **1993**, *105*, 383.
(68) Ireland, A. P.; Clark, G. W.; DeMeester, T. R. *Ann. Surg.* **1997**, 225.
(69) Blount, P. L.; Meltzer, S. J.; Yin, J.; Huang, Y.; Krasna, M. J.; Reid, B. J. *Proc. Natl. Acad. Sci. U.S.A.* **1993**, *90*, 3221.
(70) Levin, V.; Leibel, S.; Gutin, P. In *Cancer Principles & Practice of Oncology*; DeVita, V. J., Hellman, S., Rosenberg, S., Eds.; Lippincott-Raven: Philadelphia, 1997.
(71) Louis, D. N.; Cavence, W. In *Cancer Principles & Practice of Oncology*; DeVita, V. J., Hellman, S., Rosenberg, S., Eds.; Lippincott-Raven: Philadelphia, 1997.
(72) Saleman, M.; Kaplan, R. In *Comprehensive Textbook of Oncology*; Moossa, A., Robson, M., Schimpff, S., Eds.; Williams and Williams: Baltimore, 1986.
(73) Somorjai, R. L.; Dolenko, B.; Nikulin, A. K.; Pizzi, N.; Scarth, G.; Zhilkin, P.; Halliday, W.; Fewer, D.; Hill, N.; Ross, I.; West, M.; Smith, I. C.; Donnelly, S. M.; Kuesel, A. C.; Briere, K. M. *J. Magn. Reson. Imaging* **1996**, *6*, 437.
(74) Tzika, A. A.; Cheng, L. L.; Goumnerova, L.; Madsen, J. R.; Zurakowski, D.; Astrakas, L. G.; Zarifi, M. K.; Scott, R. M.; Anthony, D. C.; Gonzalez, R. G.; Black, P. M. *J. Neurosurg.* **2002**, *96*, 1023.
(75) Mountford, C. E.; Lean, C. L.; Hancock, R.; Dowd, S.; Mackinnon, W. B.; Tattersall, M. H.; Russell, P. *Invasion Metastasis* **1993**, *13*, 57.
(76) Cheng, L. L.; Chang, I.-W.; Louis, D. N.; Gonzalez, R. G. *Cancer Res.* **1998**, *58*, 1825.
(77) Leemans, C. R.; Tiwari, R.; Nauta, J. J.; van der Waal, I.; Snow, G. B. *Cancer* **1994**, *73*, 187.
(78) El-Sayed, S.; Bezabeh, T.; Odlum, O.; Patel, R.; Ahing, S.; MacDonald, K.; Somorjai, R.; Smith, I. C. P. *Head Neck* **2002**, *24*, 766.
(79) Crissman, J. D.; Liu, W. Y.; Gluckman, J. L.; Cummings, G. *Cancer* **1984**, *54*, 2995.
(80) Delikatny, E.; Hull, W.; Mountford, C. *J. Magn. Reson.* **1991**, *94*, 563.
(81) Mountford, C. E.; Doran, S.; Lean, C. L.; Russell, P. *Biophys. Chem.* **1997**, *68*, 127.
(82) May, G. L.; Wright, L. C.; Holmes, K. T.; Williams, P. G.; Smith, I. C.; Wright, P. E.; Fox, R. M.; Mountford, C. E. *J. Biol. Chem.* **1986**, *261*, 3048.
(83) Mountford, C. E.; May, G. L.; Wright, L. C.; Mackinnon, W. B.; Dyne, M.; Holmes, K. T.; van Haaften-Day, C.; Tattersall, M. H. *Lancet* **1987**, *1*, 829.
(84) Princz, E. J. Ph.D. Thesis, University of Ottawa, Ottawa, Ontario, Canada, 1998.
(85) Smith, I. C.; Princz, E. J.; Saunders: J. K. *Can. Assoc. Radiol. J.* **1990**, *41*, 32.
(86) Krupnik, E.; Briere, K. M.; Bird, R. P.; Littman, C.; Smith, I. C. *Anticancer Res.* **1999**, *19*, 1699.
(87) Carrel, S.; Sordat, B.; Merenda, C. *Cancer Res.* **1976**, *36*, 3978.
(88) Leibovitz, A.; Stinson, J. C.; McCombs, W. B.; McCoy, C. E.; Mazur, K. C.; Mabry, N. D. *Cancer Res.* **1976**, *36*, 4562.
(89) Brattain, M. G.; Marks, M. E.; McCombs, J.; Finely, W.; Brattain, D. E. *Br. J. Cancer* **1983**, *47*, 373.
(90) McBain, J. A.; Weese, J. L.; Meisner, L. F.; Wolberg, W. H.; Willson, J. K. V. *Cancer Res.* **1984**, *44*, 5813.
(91) Paraskeva, C.; Buckle, B. G.; Sheer, D.; Wigley, C. B. *Int. J. Cancer* **1984**, *34*, 49.

(92) Whitehead, R. H.; Macrae, F. A.; St. John, D. J.; Ma, J. *J. Natl. Cancer Inst.* **1985**, *74*, 759.
(93) Kirkland, S. C.; Bailey, I. G. *Br. J. Cancer* **1986**, *53*, 779.
(94) Park, J.; Oie, H. K.; Sugarbaker, P. H.; Henslee, J. G.; G-Chen, T. R.; Johnson, B. E.; Gazdar, A. *Cancer Res.* **1987**, 47.
(95) Huschtscha, L.; Bodmer, W. *In Vitro Cell. Dev. Biol.* **1990**, *26*, 743.
(96) Sze, D.; Jardetsky, I. *Biochim. Biophys. Acta* **1990**, *1054*, 198.
(97) Listinsky, J. J.; Siegal, G. P.; Listinsky, C. M. *Am. J. Clin. Pathol.* **1998**, *110*, 425.
(98) Willson, J. K. V.; Bittner, G. N.; Oberley, T. D.; Meisner, L. F.; Weese, J. L. *Cancer Res.* **1987**, 47.
(99) Paraskeva, C.; Corfield, A. P.; Harper, S.; Hague, A.; Audcent, K.; Williams, A. C. *Anticancer Res.* **1990**, *10*, 1189.
(100) Goyette, M. C.; Cho, K.; Fasching, C. L.; Levy, D. B.; Kinzler, K. W.; Paraskeva, C.; Vogelstein, B.; Stanbridge, E. J. *Mol. Cell. Biol.* **1992**, *12*, 1387.
(101) Sze, D.; Jardetzky, O. *Biochim. Biophys. Acta* **1990**, 105.
(102) Lean, C. L.; Mackinnon, W. B.; Mountford, C. E. *Magn. Reson. Med.* **1991**, *20*, 306.
(103) Nudelman, E.; Levery, S.; Kaizu, T.; Hakomori, S. *J. Biol. Chem.* **1986**, *261*, 11247.
(104) Wallace, J. C.; Raaphorst, G. P.; Somorjai, R. L.; Ng, C. E.; Fung Kee Fung, M.; Senterman, M.; Smith, I. C. *Magn. Reson. Med.* **1997**, *38*, 569.
(105) Russell, P. *Clin. Obstet. Gynaecol.* **1984**, *11*, 259.
(106) Russell, P. *Ovarian epithelial tumours with aytpical proliferation*; Churchill Livingstone: Edinburgh, Scotland, 1992.
(107) Russell, P.; Bannatyne, P. *Surgical Pathology of the Ovaries*; Churchill Livingstone: Edinburgh, Scotland, 1989.
(108) Kurhanewicz, J.; Vigneron, D. B.; Nelson, S. J. *Neoplasia (N. Y.)* **2000**, *2*, 166.
(109) Lenkinski, R. E.; Holland, G. A.; Allman, T.; Vogele, K.; Kressel, H. Y.; Grossman, R. I.; Charles, H. C.; Engeseth, H. R.; Flamig, D.; MacFall, J. R. *Radiology* **1988**, *169*, 201.
(110) Ackerman, J. J. H.; Bore, P. J.; Wong, G. G.; Gadian, D. G.; Radda, G. K. *Nature* **1980**, *283*, 167.
(111) Bottomley, P. A.; Foster, T. B.; Darrow, R. D. *J. Magn. Reson.* **1984**, *59*, 338.
(112) Frahm, J.; Merboldt, K. D.; Hanicke, W. *J. Magn. Reson.* **1987**, *72*, 502.
(113) Merboldt, K. D.; Chien, D.; Hanicke, W.; Gyngell, M. L.; Bruhn, H.; Frahm, J. *J. Magn. Reson.* **1990**, *89*, 343.
(114) Bottomley, P. A. *Ann. N. Y. Acad. Sci.* **1987**, *508*, 333.
(115) Frahm, J.; Bruhn, H.; Gyngell, M. L.; Merboldt, K. D.; Hanicke, W.; Sauter, R. *Magn. Reson. Med.* **1989**, *11*, 47.
(116) Kreis, R.; Farrow, N. A.; Ross, B. D. *Lancet* **1990**, *336*, 635.
(117) Narayana, P. A.; Johnston, D.; Flamig, D. P. *Magn. Reson. Imaging* **1991**, *9*, 303.
(118) Hennig, J.; Pfister, H.; Ernst, T.; Ott, D. *NMR Biomed.* **1992**, *5*, 193.
(119) Ross, B. D.; Kreis, R.; Ernst, T. *Eur. J. Radiol.* **1992**, *14*, 128.
(120) Barker, P. B.; Soher, B. J.; Blackband, S. J.; Chatham, J. C.; Mathews, V. P.; Bryan, R. N. *NMR Biomed.* **1993**, *6*, 89.
(121) Christiansen, P.; Henriksen, O.; Stubgaard, M.; Gideon, P.; Larsson, H. B. W. *Magn. Reson. Imaging* **1993**, *11*, 107.
(122) Kreis, R.; Ernst, T.; Ross, B. D. *J. Magn. Reson.* **1993**, *102*, 9.
(123) Michaelis, T.; Merboldt, K. D.; Bruhn, H.; Hanicke, W.; Frahm, J. *Radiology* **1993**, *187*, 219.
(124) Danielsen, E.; Henriksen, O. *NMR Biomed.* **1994**, *7*, 311.
(125) Heerschap, A.; van den Berg, P. *Proceedings of the 12th Annual Meeting of the Society of Magnetic Resonance in Medicine*, New York, 1993; p 318.
(126) Kreis, R.; Ernst, T.; Ross, B. D. *Magn. Reson. Med.* **1993**, *30*, 1.
(127) Ross, B.; Bluml, S. *Anat. Rec.* **2001**, *265*, 54.
(128) Langkowski, J. H.; Wieland, J.; Bomsdorf, H.; Leibfritz, D.; Westphal, M.; Offermann, W.; Maas, R. *Magn. Reson. Imaging* **1989**, *7*, 547.
(129) Posse, S.; Schuknecht, B.; Smith, M.; van Zijl, P.; Herschkowitz, N.; Moonen, T. *J. Comput. Assist. Tomogr.* **1993**, *17*, 1.
(130) Fulham, M. J.; Bizzi, A.; Dietz, M. J.; Shih, H. H.; Raman, R.; Sobering, G. S.; Frank, J. A.; Dwyer, A. J.; R., A. J.; G, D. C. *Radiology* **1992**, *185*, 675.
(131) Luyten, P. R.; Marien, A. J.; Heindel, W.; van, G. P.; Herholz, K.; den, H. J.; Friedmann, G.; Heiss, W. D. *Radiology* **1990**, *176*, 791.
(132) van, Z. P.; Moonen, C. T.; Gillen, J.; Daly, P. F.; Miketic, L., S.; Frank, J. A.; DeLaney, T. F.; Kaplan, O.; Cohen, J. S. *NMR Biomed.* **1990**, *3*, 227.
(133) Kurhanewicz, J.; Vigneron, D. B.; Males, R. G.; Swanson, M. G.; Yu, K. K.; Hricak, H. *Radiol. Clin. North Am.* **2000**, *38*, 115−138, viii−ix.
(134) Nelson, S.; McKnight, T. R.; Henry, R. G. *Neuroimaging Clin. North Am.* **2002**, *12*, 599.
(135) Majos, C.; Alonso, J.; Aguilera, C.; Serrallonga, M.; Coll, S.; Acebes, J.; Arus, C.; Gili, J. *Diagn. Neuroradiol.* **2003**, *45*, 129.
(136) Majos, C.; Alonso, J.; Aguilera, C.; Serrallonga, M.; Coll, S.; Acebes, J. J.; Arus, C.; Gili, J. *Neuroradiology* **2003**, *45*, 129.
(137) Majos, C.; Alonso, J.; Aguilera, C.; Serrallonga, M.; Perez-Martin, J.; Acebes, J. J.; Arus, C.; Gili, J. *Eur. Radiol.* **2003**, *13*, 582.
(138) Majos, C.; Alonso, J.; Aguilera, C.; Serrallonga, M.; Acebes, J. J.; Arus, C.; Gili, J. *Radiology* **2002**, *225*, 556.
(139) Bulakbasi, N.; Kocaoglu, M.; Ors, F.; Tayfun, C.; Ucoz, T. *Am. J. Neuroradiol.* **2003**, *24*, 225.
(140) Herminghaus, S.; Pilatus, U.; Moller-Hartmann, W.; Raab, P.; Lanfermann, H.; Scholote, W.; E., Z. F. *NMR Biomed.* **2002**, *15*, 385.
(141) Jayasundar, R.; Singh, V. P. *Neurol. India* **2002**, *50*, 436.
(142) Murphy, M.; Loosemore, A.; Clifton, A. G.; Howe, F. A.; Tate, A. R.; Cudlip, S. A.; Wilkins, P. R.; Griffiths, J. R.; Bell, B., A. *Br. J. Neurosurg.* **2002**, *16*, 329.
(143) Kubas, B.; Tarasow, E.; Dzienis, W.; Lebkowski, W.; Zimnoch, L.; Dzieciol, J.; Siergiejczyk, L.; Walecki, J.; Lewko, J. *Neurol. Neurochir. Pol.* **2001**, *5*, 90.
(144) Leclerc, X.; Huisman, T. A.; Sorensen, A. G. *Curr. Opin. Oncol.* **2002**, *14*, 292.
(145) McKnight, T. R.; Noworolski, S. M.; Vigneron, D. B.; Nelson, S. J. *J. Magn. Reson. Imaging* **2001**, *13*, 167.
(146) Rand, S.; Prost, R.; Haughton, V.; Mark, L.; Strainer, J.; Johansen, J.; Kim, T.; Chetty, V.; Mueller, W.; Meyer, G.; Krouwer, H. *Am. J. Neuroradiol.* **1997**, *18*, 1695.
(147) Krouwer, H. G.; Kim, T. A.; Rand, S. D. *Am. J. Neuroradiol.* **1998**, *19*, 1695.
(148) Arnold, D.; Emrich, J.; Shoubridge, E.; Villemure, J.; Feindel, W. *J. Neurosurg.* **1991**, *74*, 447.
(149) Arnold, D.; Shoubridge, E.; Feindel, W.; Villemure, J. *Can. J. Neurol. Sci.* **1987**, *14*, 570.
(150) Preul, M.; Caramanos, Z.; Collins, D.; Villemure, J.; Leblanc, R.; Olivier, A.; Pokrupa, R.; Arnold, D. *Nat. Med.* **1996**, *2*, 323.
(151) Preul, M. C.; Caramanos, Z.; Leblanc, R.; Villemure, J. G.; Arnold, D. L. *NMR Biomed.* **1998**, *11*, 192.
(152) Mountford, C. E.; Siddall, P. J.; Stanwell, P. T.; Somorjai, R. L.; Dolenko, B.; Nikulin, S.; Himmelreich, U.; Lean, C. L.; Woodhouse, A.; Cousins, M. J. *Proceedings, 12th Scientific Meeting, International Society for Magnetic Resonance in Medicine*: Kyoto, Japan, 2004; p 2430.
(153) Ross, B.; Danielsen, E. *Magnetic Resonance Spectroscopy: Diagnosis of Neurological Diseases*; Marcel Dekker: New York, 1999.
(154) Han, M.; Partin, A.; Plantadosi, S.; Epstein, J.; Walsh, P. *J. Urol.* **2001**, *166*, 416.
(155) Schnall, M.; Lenkinski, R.; Pollack, H.; Imai, Y.; Kressel, H. *Radiology* **1989**, *172*, 570.
(156) Chelsky, M.; Schnall, M.; Seidmon, E.; Pollack, H. *J. Urol.* **1993**, *150*, 391.
(157) Hricak, H.; White, S.; Vigneron, D.; Kurhanewicz, J.; Kosco, A.; Levin, D.; Weiss, J.; Narayan, P.; Carroll, P. R. *Radiology* **1994**, *193*, 703.
(158) Kurhanewicz, J.; Vigneron, D. B.; Nelson, S. J.; Hricak, H.; MacDonald, J. M.; Konety, B.; Narayan, P. *Urology* **1995**, *45*, 459.
(159) Thomas, M.; Narayan, P.; Kurhanewicz, J.; Jajodia, P.; Weiner, M. *J. Magn. Reson.* **1990**, *87*, 610.
(160) Schick, F.; Bongers, H.; Kurz, S.; Jung, W. I.; Pfeffer, M.; Lutz, O. *Magn. Reson. Med.* **1993**, *29*, 38.
(161) Kim, J. K.; Kim, D. Y.; Lee, Y. H.; Sung, N. K.; Chung, D. S.; Kim, O. D.; Kim, K. B. *Magn. Reson. Imaging* **1998**, *16*, 1281.
(162) Heerschap, A.; Jager, G. J.; van der Graaf, M.; Barentsz, J. O.; de la Rosette, J. J.; Oosterhof, G. O.; Ruijter, E. T.; Ruijs, S. H. *Anticancer Res.* **1997**, *17*, 1455.
(163) Zakian, K. L.; Sircar, K.; Kleinman, S.; Shukla-Dave, A.; Kattan, M. W.; Hricak, H. *Proceedings, RSNA, Radiological Society of North America, 88th Scientific Assembly and Annual Meeting*, McCormick Place, Chicago, 2002; p 268.
(164) Boetes, C.; Barentsz, J. O.; Mus, R. D.; van der Sluis, R. F.; van Erning, L. J.; Hendriks, J. H.; Holland, R.; Ruys, S., H *Radiology* **1994**, *193*, 777.
(165) Kuhl, C. K.; Mielcareck, P.; Klaschik, S.; Leutner, C.; Wardelmann, E.; Gieseke, J.; Schild, H. H. *Radiology* **1999**, *211*, 101.
(166) Kvistad, K. A.; Rydland, J.; Vainio, J.; Smethurst, H. B.; Lundgren, S.; Fjosne, H. E.; Haraldseth, O. *Radiology* **2000**, *216*, 545.
(167) Stomper, P.; Herman, S.; Klippenstein, D. L.; Winston, J. S.; Edge, S. B.; Arredondo, M. A.; Mazurchuk, R. V.; Blumenson, L. E. *Radiology* **1995**, *197*, 387.
(168) Fischer, U.; Kopka, L.; Grabbe, E. *Radiology* **1999**, *213*, 881.
(169) Kinkel, K.; Hylton, N. *J. Magn. Reson. Imaging* **2001**, *13*, 821.
(170) Heywang-Kobrunner, S. *Invest. Radiol.* **1994**, *29*, 94.
(171) Kaiser, W. A.; Zeitler, E. *Radiology* **1989**, *170*, 681.
(172) Kuhl, C. K.; Kreft, B. P.; Bieling, H. B.; Gieseke, J.; Sommer, T.; Lutterbey, G.; Schild, H. H. *Radiology* **1997**, *203*, 137.
(173) Padhani, A. R. *J. Magn. Reson. Imaging* **2002**, *16*, 407.
(174) Sijens, P. E.; Wijrdeman, H. K.; Moerland, M. A.; Bakker, C. J.; Vermeulen, J. W.; Luyten, P. R. *Radiology* **1988**, *169*, 615.
(175) Roebuck, J. R.; Cecil, K. M.; Schnall, M. D.; Lenkinski, R. E. *Radiology* **1998**, *209*, 269.
(176) Masood, S. *Diagn. Cytopathol.* **1995**, *13*, 388.

(177) Yeung, D. K. W.; Cheung, H. S.; Tse, G. M. K. *Radiology* **2001**, *220*, 40.
(178) Kvistad, K. A.; Bakken, I. J.; Gribbestad, I. S.; Ehrnholm, B.; Lundgren, S.; Fjosne, H. E.; Haraldseth, O. *J. Magn. Reson. Imaging* **1999**, *10*, 159.
(179) Cecil, K. M.; Schnall, M. D.; Siegelman, E. S.; Lenkinski, R. E. *Breast Cancer Res. Treat.* **2001**, *68*, 45.
(180) Jagannathan, N. R.; Kumar, M.; Seenu, V.; Coshic, O.; Dwivedi, S. N.; Julka, P. K.; Srivastava, A.; Rath, G. K. *Br. J. Cancer* **2001**, *84*, 1016.
(181) Stanwell, P.; Gluch, L.; Clark, D.; Lean, C.; Giuffre, B.; Malycha, P.; Tomanek, B.; Mountford, C. Unpublished data.
(182) Nicolau, C.; Dietrich, W.; Steiner, M. R.; Steiner, S.; Melnick, J. L. *Biochim. Biophys. Acta* **1975**, *382*, 311.
(183) Katz-Brull, R.; Lavin, P.; Lenkinski, R. *J. Natl. Cancer Inst.* **2002**, *94*, 1197.
(184) King, S. B.; Ryner, L. N.; Tomanek, B.; Sharp, J. C.; Smith, I. C. *Magn. Reson. Med.* **1999**, *42*, 655.
(185) Ryner, L. N.; Sorenson, J. A.; Thomas, M. A. *J. Magn. Reson.* **1995**, *107*, 126.
(186) Thomas, M.; Yue, K.; Binesh, N.; Davanzo, P.; Kumar, A.; Siegel, B.; Frye, M.; Curran, J.; Lufkin, R.; Martin, P.; Guze, B. *Magn. Reson. Med.* **2001**, *46*, 58.
(187) Thomas, M. A.; Bines, N.; Yu, K.; DeBruh, N. *J. Magn. Reson. Imaging* **2001**, *14*, 181.
(188) Binesh, N.; Yue, K.; Fairbanks, L.; Thomas, M. A. *Magn. Reson. Med.* **2002**, *48*, 942.
(189) Yue, K.; Marumoto, A.; Binesh, N.; Thomas, M. A. *Magn. Reson. Med.* **2002**, *47*, 1059.
(190) Bourne, R.; Katelaris, P.; Danieletto, S.; Dzendrowskyj, T.; Stanwell, P.; Mountford, C. *ANZ J. Surg.* **2003**, *73*, 666.
(191) Somorjai, R. L.; Dolenko, B.; Halliday, W.; Fowler, D.; Hill, N.; Ross, I.; Brière, K. M.; Smith, I. C. P. *J. Med. Biochem.* **1999**, *3*, 17.
(192) Menard, C.; Smith, I. C.; Somorjai, R. L.; Leboldus, L.; Patel, R.; Littman, C.; Robertson, S. J.; Bezabeh, T. *Int. J. Radiat. Oncol., Biol., Phys.* **2001**, *50*, 317.
(193) Doran, S.; Falk, G.; Somorjai, R.; Lean, C.; Himmelreich, U.; Philips, J.; Russell, P.; Dolenko, B.; Nikulin, A.; Mountford, C. *Am. J. Surg.* **2003**, *185*, 232.
(194) Bourne, R.; Thompson, J.; Scolyer, R.; Stretch, J.; Li, L.; Dzendrowskyj, T.; Dolenko, B.; Somorjai, R.; Mountford, C.; Lean, C. *Proceedings, 11th Scientific Meeting, International Society for Magnetic Resonance in Medicine, ISMRM*, Toronto, Canada, 2003; p 1302.
(195) Mountford, C.; Siddall, P.; Woodhouse, A.; Stanwell, P.; Somorjai, R. Provisional Patent Serial No. 10/437,406, 2003.
(196) Bezabeh, T.; Samy, E.; Patel, R.; Somorjai, R.; Bramwell, V.; Kandel, R.; Smith, I. C. P. *Sarcoma* **2002**, *6*, 97.

CR030410G